Table 2. Body weights and histopathologic evaluation of gastritis in Mongolian gerbils and mice in experiment II

Animal	Group (*n*)	Treatment	BW (g)	Scores of gastritis			
				Infiltration of neutrophils		Infiltration of mononuclear cells	
				Antrum	Corpus	Antrum	Corpus
Gerbils	G (10)	Hp + 10 ppm PS	76.4 ± 4.5	2.3 ± 0.5	1.6 ± 0.9	2.4 ± 0.4	1.9 ± 0.5
	H (10)	Hp + 3 ppm PS	74.2 ± 10.6	2.2 ± 0.4	1.9 ± 1.1	2.5 ± 0.5	2.0 ± 0.8
	I (10)	Hp + 1 ppm PS	74.3 ± 7.7	2.4 ± 0.4	1.6 ± 0.8	2.5 ± 0.4	2.0 ± 0.8
	J (10)	Hp	70.8 ± 8.2	2.3 ± 0.4	1.2 ± 0.9	2.7 ± 0.2	1.7 ± 0.7
	K (8)	Broth + 10 ppm PS	73.8 ± 4.2	0.0 ± 0.0	0.0 ± 0.0	0.1 ± 0.2	0.1 ± 0.2
	L (10)	Broth	75.2 ± 6.4	0.1 ± 0.2	0.0 ± 0.0	0.2 ± 0.2	0.0 ± 0.0
Mice	M (19)	Hp + 10 ppm PS	30.2 ± 2.2	1.0 ± 0.3	1.3 ± 0.6	0.9 ± 0.2	1.2 ± 0.4
	N (19)	Hp + 3 ppm PS	30.5 ± 2.0	1.1 ± 0.3	1.4 ± 0.4	1.0 ± 0.2	1.3 ± 0.4
	O (19)	Hp + 1 ppm PS	30.4 ± 1.8	0.8 ± 0.3	1.0 ± 0.5	0.8 ± 0.3	1.1 ± 0.5
	P (20)	Hp	28.9 ± 2.8	1.0 ± 0.5	1.2 ± 0.6	0.8 ± 0.3	1.0 ± 0.5
	Q (21)	Broth + 10 ppm PS	29.2 ± 1.8	0.0 ± 0.1	0.2 ± 0.3	0.0 ± 0.0	0.0 ± 0.1
	R (20)	Broth	28.4 ± 1.0	0.1 ± 0.2	0.4 ± 0.5	0.0 ± 0.0	0.0 ± 0.0

NOTE: Values for results are expressed as mean ± SD.

Statistical analysis

The Fisher's exact test was used to assess incidences of gastric adenocarcinomas. Quantitative values were expressed as mean ± SD or SE, and differences between means were statistically analyzed by the ANOVA or Kruskal-Wallis followed by the multiple comparison test. P values of <0.05 were considered to be statistically significant.

Results

Average body weights, titer of anti-*H. pylori* antibodies, and relative organ weights

Data for average body weights, titer of anti-*H. pylori* antibodies, and relative organ weights in the long-term experiment (experiment I) and average body weights in the short-term experiment (experiment II) are shown in Tables 1 and 2, respectively. There was no significant variation of body weights in experiments I and II. In experiment I, all *H. pylori*–infected groups (groups A-D) showed significantly higher values for anti-*H. pylori* antibody titers than the noninfected group (group E). The relative liver weights in groups A to D were markedly higher than in nontreated control group (group F). The relative kidney weights in group E were statistically decreased compared with group F. In internal organs other than the stomach, including the liver, kidney, spleen, heart, and lung of all groups (groups A-F), no macroscopic or microscopic lesions were observed.

Status of gastritis

All gastric mucosal specimens from uninfected gerbils and mice had normal histomorphology (Fig. 1C, *a*). Histologic findings for chronic gastritis in experiments I (Table 3) and II (Table 2) are summarized. The long-term *H. pylori*–infected gerbils showed severe gastritis with intestinal metaplasia and HPGs (Fig. 1C, *b*). There were no significant differences in inflammatory scores, including infiltration of neutrophils or mononuclear cells, intestinal metaplasia, and HPGs, both in the antrum and corpus, among all infected groups in experiment I. In experiment II, the infiltration of neutrophils and mononuclear cells of short-term *H. pylori*–infected gerbils was greater than that in mice. There were no statistically significant differences in the degree of inflammation among *H. pylori*–infected animals, as in experiment I. In experiment I, the score for iNOS immunohistochemistry in group A (*H. pylori* + MNU + 10 ppm pitavastatin) was markedly higher than that in group D (*H. pylori* + MNU) both in the antrum and corpus (Fig. 1C, *c* and *d*).

Incidences of glandular stomach adenocarcinomas

In experiment I, both well-differentiated and poorly differentiated adenocarcinomas were found in *H. pylori*–infected and MNU-treated groups (groups A-D) at 52 weeks after infection (Fig. 1C, *e* and *f*). However, there were no significant differences in the incidences among groups A to D [group A, 45.0% (18 of 40); group B, 56.4% (22 of 39); group C, 50.0% (20 of 40); group D, 41.5% (17 of 41); Table 1]. In noninfected control groups (groups E and F) and short-term infected groups (experiment II), no tumors developed in the stomach.

Serologic results

On serologic examination, pitavastatin treatment significantly increased serum T-Chol, TG, and LDL levels in *H. pylori*–infected gerbils in a dose-dependent manner (groups A-D) in the long-term experiment (experiment I; Fig. 2). Similarly, in noninfected animals (groups E and F), serum LDL levels were increased by 10 ppm pitavastatin treatment. On the other hand, HDL levels were markedly reduced in both group D (*H. pylori* + MNU) and group E (10 ppm pitavastatin) compared with group F (untreated control).

In experiment II, serum TG and HDL levels showed significant up-regulation by pitavastatin treatment in *H. pylori*–infected gerbils (groups G-J). In contrast, T-Chol and HDL

levels were markedly decreased by 10 ppm pitavastatin in noninfected gerbils (groups K and L). In *H. pylori*–infected mice (groups M-P), serum TG levels were significantly increased by pitavastatin, as in the gerbil case. In noninfected mice (groups Q and R), the serum LDL level showed a tendency for decrease with 10 ppm pitavastatin treatment, although this was not statistically significant ($P = 0.063$).

Administration of pitavastatin and mRNA expression of IL-1β, TNF-α, and iNOS

Gastric IL-1β, TNF-α, and iNOS mRNA were found to be expressed at very low levels in the noninfected control gerbils. However, in the *H. pylori*–infected animals, the levels of these inflammatory factors were markedly elevated in the antrum and corpus (Fig. 3A and B). In the long-term experiment (experiment I), relative expression of IL-1β and TNF-α in the antrum of pitavastatin-treated groups (groups A-C) was significantly up-regulated compared with the untreated group (group D; Fig. 3A).

Discussion

The present study did not provide any evidence of statin protection against gastritis or gastric carcinogenesis in two animal models. The relationship between statin use and cancer incidence has been evaluated in numerous epidemiologic studies. Some reports supported a role in cancer chemoprevention (6, 28), and others refuted the hypothesis (29). Recently, Lubet et al. (30) suggested that atorvastatin and lovastatin fail to inhibit mammary carcinogenesis of rodents. In case of gastrointestinal cancer, clinical studies of statins for preventive effects have also produced conflicting results (31). Statins are the most widely used drugs both in the amounts prescribed and the proceeds of sales (32), so we need to clarify whether they are truly effective for cancer chemoprevention. Here, we showed that *H. pylori*–associated gastric carcinogenesis in Mongolian gerbils is not prevented by oral administration of pitavastatin at 10 ppm in the diet. We selected the pitavastatin as a strong candidate to alleviate gastritis and gastric carcinogenesis as well as to lower the serum lipid levels because pitavastatin has more potent lipid-lowering effects than pravastatin, simvastatin, and atorvastatin (21, 33). Furthermore, pitavastatin has been known to be minimally affected by cytochrome *P*450 3A4 inhibitors unlike simvastatin, lovastatin, and atorvastatin (34). Because cytochrome *P*450 metabolisms in gerbils have not been fully clarified yet, we selected pitavastatin to avoid species difference in the drug metabolism in this experiment. Among mice strains, C57BL/6 mice showed excellent colonization of *H. pylori* in the antrum, whereas BALB/c and CBA mice showed only mild gastritis (35); thus, the former was chosen here. Pitavastatin has been shown to prevent digestive system carcinogenesis, such as colorectal and lingual cancer, in mouse models (14, 36); however, the degree of gastritis in our study was not attenuated by pitavastatin in *H. pylori*–infected gerbils and mice. The major determining factor of stomach carcinogenesis is the severity of *H. pylori*–induced gastritis (37). Therefore, the ineffectiveness of pitavastatin regarding prevention of gastric cancer development in the gerbil model might be due to the lack of suppressive effects on *H. pylori*–induced gastritis.

In the long-term experiment, interestingly, our data suggested that the serum lipid levels (T-Chol, TG, and LDL) of *H. pylori*–infected and MNU-treated gerbils were significantly increased by pitavastatin in a dose-dependent manner. In noninfected gerbils, similarly, values for LDL cholesterol level were markedly elevated by the statin, although the HDL cholesterol level was significantly decreased. It was expected that pitavastatin would lower the LDL without changing HDL levels. Therefore, we did the additional short-term experiment (experiment II) to clarify whether the effect of pitavastatin on serum lipid profile was influenced by *H. pylori* infection, MNU treatment, or biological trait of gerbils. Again, inflammatory

Table 3. Histopathologic evaluation of gastritis in Mongolian gerbils in experiment I

Group (*n*)	Treatment	Infiltration of neutrophils		Infiltration of mononuclear cells		Intestinal metaplasia		HPGs		COX-2 immunostaining		iNOS immunostaining	
		Antrum	Corpus	Antrum	Corpus	Antrum	Corpus	Antrum	Corpus	Antrum	Corpus	Antrum	Corpus
A (40)	Hp + MNU + 10 ppm PS	2.0±0.7	2.3±0.8	2.8±0.4	2.6±0.5	1.2±0.8	1.6±0.8	2.3±0.7	2.2±0.9	1.3±0.7	1.6±0.7	2.0±0.6*	1.8±0.6*
B (39)	Hp + MNU + 3 ppm PS	2.1±0.6	2.4±0.8	2.7±0.4	2.5±0.5	1.3±0.8	1.5±0.6	2.3±0.7	2.3±0.7	1.5±0.8	1.7±0.7	1.7±0.5	1.7±0.6
C (40)	Hp + MNU + 1 ppm PS	2.0±0.7	2.3±0.7	2.7±0.4	2.5±0.6	1.3±0.9	1.6±0.8	2.3±0.6	2.0±0.9	1.5±0.7	1.6±0.7	1.6±0.6	1.4±0.5
D (41)	Hp + MNU	1.8±0.6	2.1±0.8	2.6±0.5	2.4±0.5	1.0±0.7	1.2±0.7	2.1±0.7	1.9±0.8	1.6±0.8	1.5±0.6	1.5±0.6	1.4±0.5
E (10)	Broth + 10 ppm PS	0.0±0.0	0.0±0.0	0.3±0.4	0.0±0.0	0.0±0.0	0.0±0.0	0.0±0.0	0.0±0.0	0.0±0.0	0.0±0.0	0.1±0.3	0.0±0.0
F (5)	Untreated control	0.0±0.0	0.0±0.0	0.0±0.0	0.0±0.0	0.0±0.0	0.0±0.0	0.0±0.0	0.0±0.0	0.0±0.0	0.0±0.0	0.0±0.0	0.0±0.0

NOTE: Values for results are expressed as mean ± SD.
*$P < 0.01$ versus group D.

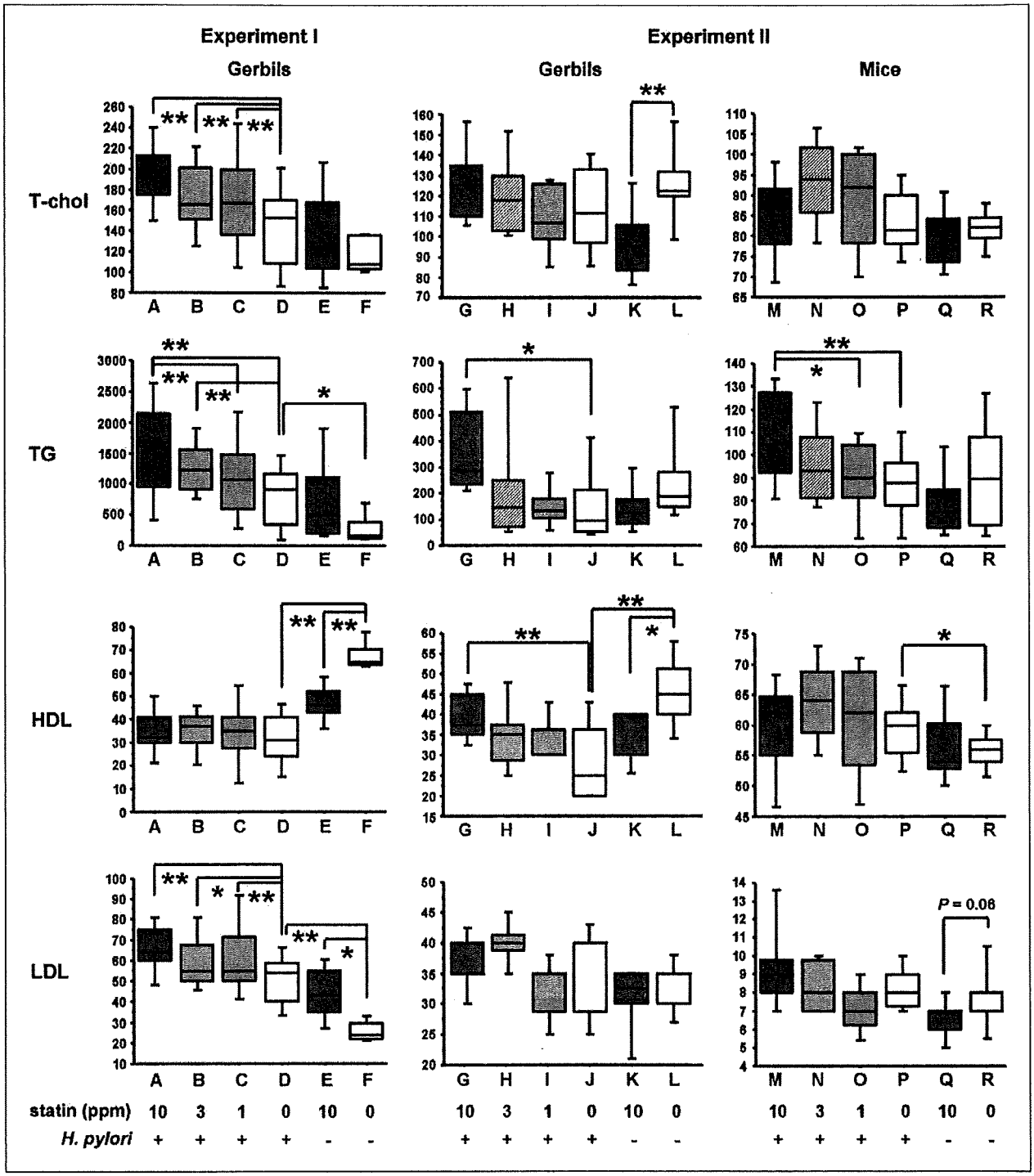

Fig. 2. Serologic results were depicted by box plots. *Line inside each box*, median; *boxes*, 25th and 75th percentiles; *error bars*, 90th and 10th percentiles. *, $P < 0.05$; **, $P < 0.01$.

scores for gastritis in *H. pylori*–infected gerbils and mice were not attenuated by pitavastatin, and serum TG levels were significantly increased. On the other hand, in the noninfected mice, LDL cholesterol showed tendency for decrease. Similarly, in noninfected gerbils, pitavastatin significantly reduced the serum T-Chol and HDL levels. These serologic results suggest that *H. pylori* infection might influence the effects of the statin. Oral administrated pitavastatin is absorbed mainly in the

duodenum and colon with a minimum metabolic change but partly in the stomach. Thus, there is a possibility that the pharmacokinetics of pitavastatin might be modified by *H. pylori*–induced severe chronic gastritis.

Some infectious diseases, such as *Chlamydia pneumoniae* infection, have been considered as risk factors for coronary heart disease (18), and several studies have pointed to an association between *H. pylori* infection and vascular changes due to the alteration of the serum lipid profile (19, 38). Previous studies reported that the serum T-Chol, TG, or LDL concentrations in *H. pylori*–infected persons are significantly elevated over those in noninfected individuals (39, 40). On the other hand, several authors described HDL cholesterol levels to be decreased by long-term infection with *H. pylori* (41–43). In the present study, *H. pylori*–infected animals showed similar lipid dynamics with significant elevation of TG and LDL and depression of HDL, and pitavastatin markedly up-regulated the T-Chol and TG levels in infected groups. Thus, our data support the hypothesis that the conversion of serum lipid dynamics caused by *H. pylori* infection influences the cholesterol-lowering effect of pitavastatin.

The antral mRNA expression levels of inflammatory cytokines (IL-1β and TNF-α) were found to be significantly increased by pitavastatin treatment in *H. pylori*–infected and MNU-treated gerbils, although there were no significant differences in inflammatory scores. In addition, the immunoreactivity scores of iNOS both in the antrum and corpus of these gerbils were higher than those of control (*H. pylori* + MNU) gerbils. Recently, Habara et al. (44) showed that pitavastatin up-regulates iNOS expression in cytokine-stimulated hepatocytes. The findings described here suggest potential enhancing effects of statins on *H. pylori*–induced gastritis through up-regulation of these inflammatory factors, in contrast to the anti-inflammatory effects reported in colon.

Statins are well recognized as relatively safe drugs, although adverse effects include hepatotoxicity and myopathy at low incidence. In the present study, there was no significant variation in body weights with pitavastatin treatment in either *H. pylori*–infected or noninfected animals. No macroscopic lesions in the liver, spleen, kidney, heart, lung, pancreas, testis, and skeletal muscles were observed. In addition, histologic examination revealed no pathologic findings in the liver, spleen, kidney, heart, lung, and skeletal muscles

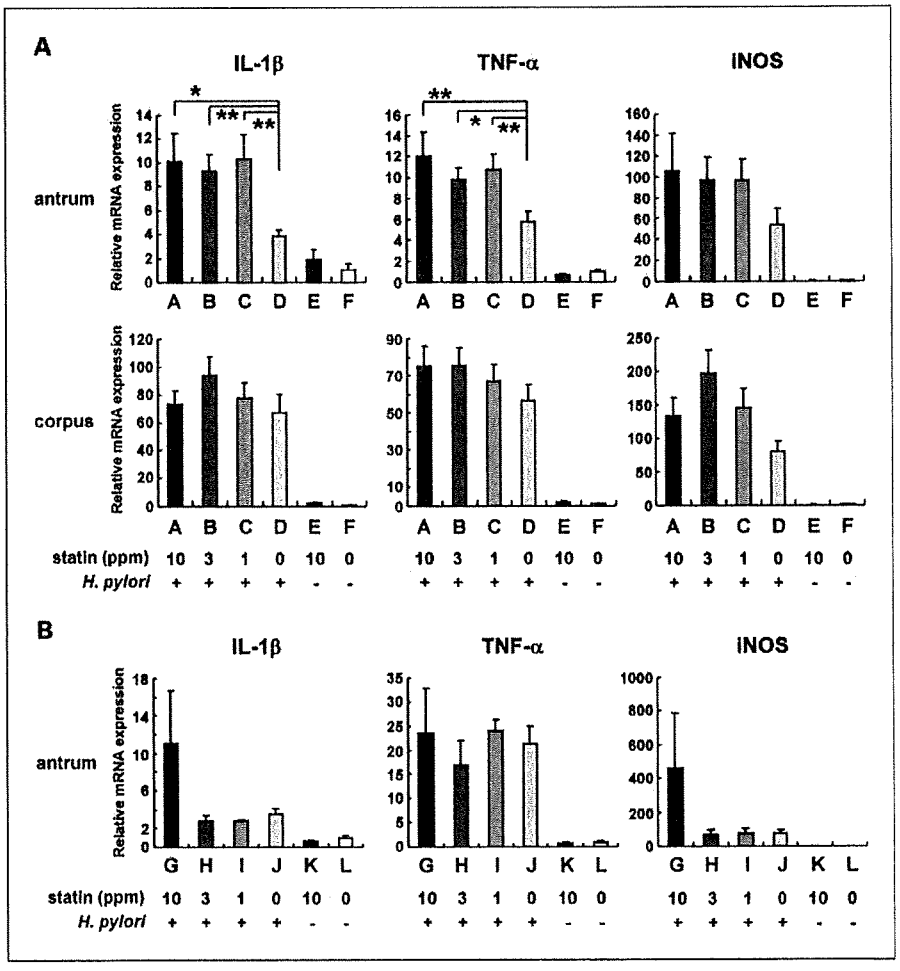

Fig. 3. Relative expression levels of IL-1β, TNF-α, and iNOS mRNAs in the gastric mucosa. *A*, expression in the antrum and corpus of gerbils at 52 wk after infection. Columns, mean arbitrary units relative to 1.0 for controls (group F); bars, SE. Note increase in groups A to C (pitavastatin-treated groups) compared with group D (*H. pylori*–infected control group), especially in the antrum. *, $P < 0.05$; **, $P < 0.01$. *B*, expression levels in the antrum of glandular stomachs of gerbils at 12 wk after infection. Columns, mean arbitrary units relative to 1.0 for controls (group L); bars, SE. Note increase in group G (10 ppm pitavastatin–treated gerbils) compared with group J (*H. pylori*–infected control gerbils), although statistically significant differences are lacking among groups G to J.

of gerbils at 52 weeks. Therefore, it was considered that pitavastatin toxicity was lacking or limited at the dose used in the present study.

In conclusion, pitavastatin does not seem to be associated with reduced risk of stomach carcinogenesis in *H. pylori*–infected Mongolian gerbils. Furthermore, *H. pylori* infection interferes with the serum lipid-lowering effects of pitavastatin in gerbil and mouse models. Our results therefore suggest that care is needed in use of statins for *H. pylori*–infected individuals, especially those with severe chronic gastritis. Large-scale epidemiologic studies should be recommended to determine whether statins have effects on stomach cancer development.

Disclosure of Potential Conflicts of Interest

No potential conflicts of interest were disclosed.

References

1. Hebert PR, Gaziano JM, Chan KS, Hennekens CH. Cholesterol lowering with statin drugs, risk of stroke, and total mortality. An overview of randomized trials. JAMA 1997;278:313–21.
2. Baigent C, Keech A, Kearney PM, et al. Efficacy and safety of cholesterol-lowering treatment: prospective meta-analysis of data from 90,056 participants in 14 randomised trials of statins. Lancet 2005;366:1267–78.
3. Dulak J, Jozkowicz A. Anti-angiogenic and anti-inflammatory effects of statins: relevance to anti-cancer therapy. Curr Cancer Drug Targets 2005;5:579–94.
4. Ito MK, Talbert RL, Tsimikas S. Statin-associated pleiotropy: possible beneficial effects beyond cholesterol reduction. Pharmacotherapy 2006;26: 85–101S.
5. Poynter JN, Gruber SB, Higgins PD, et al. Statins and the risk of colorectal cancer. N Engl J Med 2005;352:2184–92.
6. Demierre MF, Higgins PD, Gruber SB, Hawk E, Lippman SM. Statins and cancer prevention. Nat Rev Cancer 2005;5:930–42.
7. Chan KK, Oza AM, Siu LL. The statins as anticancer agents. Clin Cancer Res 2003;9:10–9.
8. Coogan PF, Smith J, Rosenberg L. Statin use and risk of colorectal cancer. J Natl Cancer Inst 2007; 99:32–40.
9. Browning DR, Martin RM. Statins and risk of cancer: a systematic review and metaanalysis. Int J Cancer 2007;120:833–43.
10. Dale KM, Coleman CI, Henyan NN, Kluger J, White CM. Statins and cancer risk: a meta-analysis. JAMA 2006;295:74–80.
11. Jacobs EJ, Rodriguez C, Brady KA, Connell CJ, Thun MJ, Calle EE. Cholesterol-lowering drugs and colorectal cancer incidence in a large United States cohort. J Natl Cancer Inst 2006;98:69–72.
12. Vinogradova Y, Hippisley-Cox J, Coupland C, Logan RF. Risk of colorectal cancer in patients prescribed statins, nonsteroidal anti-inflammatory drugs, and cyclooxygenase-2 inhibitors: nested case-control study. Gastroenterology 2007;133: 393–402.
13. Parkin DM, Bray F, Ferlay J, Pisani P. Global cancer statistics, 2002. CA Cancer J Clin 2005;55:74–108.
14. Yasui Y, Suzuki R, Miyamoto S, et al. A lipophilic statin, pitavastatin, suppresses inflammation-associated mouse colon carcinogenesis. Int J Cancer 2007;121:2331–9.
15. Swamy MV, Patlolla JM, Steele VE, Kopelovich L, Reddy BS, Rao CV. Chemoprevention of familial adenomatous polyposis by low doses of atorvastatin and celecoxib given individually and in combination to APCMin mice. Cancer Res 2006;66: 7370–7.
16. Uemura N, Okamoto S, Yamamoto S, et al. *Helicobacter pylori* infection and the development of gastric cancer. N Engl J Med 2001;345:784–9.
17. IARC Working Group on the Evaluation of Carcinogenic Risks to Humans Infection with *Helicobacter pylori*. Schistosomes, liver flukes and *Helicobacter pylori*. In: IARC monographs on the evaluation of carcinogenic risks to humans, vol. 61. Lyon: World Health Organization/International Agency for Research on Cancer; 1994. p. 177–241.
18. Patel P, Mendall MA, Carrington D, et al. Association of *Helicobacter pylori* and *Chlamydia pneumoniae* infections with coronary heart disease and cardiovascular risk factors. BMJ 1995;311:711–4.
19. Niemela S, Karttunen T, Korhonen T, et al. Could *Helicobacter pylori* infection increase the risk of coronary heart disease by modifying serum lipid concentrations? Heart 1996;75:573–5.
20. Sugiyama A, Maruta F, Ikeno T, et al. *Helicobacter pylori* infection enhances *N*-methyl-*N*-nitrosourea-induced stomach carcinogenesis in the Mongolian gerbil. Cancer Res 1998;58:2067–9.
21. Mukhtar RY, Reid J, Reckless JP. Pitavastatin. Int J Clin Pract 2005;59:239–52.
22. Shimizu N, Inada KI, Tsukamoto T, et al. New animal model of glandular stomach carcinogenesis in Mongolian gerbils infected with *Helicobacter pylori* and treated with a chemical carcinogen. J Gastroenterol 1999;34:61–6.
23. Dixon MF, Genta RM, Yardley JH, Correa P. Classification and grading of gastritis. The updated Sydney System. International Workshop on the Histopathology of Gastritis, Houston 1994. Am J Surg Pathol 1996;20:1161–81.
24. Tanaka T, Kohno H, Suzuki R, et al. Dextran sodium sulfate strongly promotes colorectal carcinogenesis in Apc(Min/+) mice: inflammatory stimuli by dextran sodium sulfate results in development of multiple colonic neoplasms. Int J Cancer 2006; 118:25–34.
25. Zingarelli B, Szabo C, Salzman AL. Reduced oxidative and nitrosative damage in murine experimental colitis in the absence of inducible nitric oxide synthase. Gut 1999;45:199–209.
26. Cao X, Tsukamoto T, Seki T, et al. 4-Vinyl-2,6-dimethoxyphenol (canolol) suppresses oxidative stress and gastric carcinogenesis in *Helicobacter pylori*-infected carcinogen-treated Mongolian gerbils. Int J Cancer 2008;122:1445–54.
27. Tsukamoto T, Fukami H, Yamanaka S, et al. Hexosaminidase-altered aberrant crypts, carrying decreased hexosaminidase α and β subunit mRNAs, in colon of 1,2-dimethylhydrazine-treated rats. Jpn J Cancer Res 2001;92:109–18.
28. Karp I, Behlouli H, Lelorier J, Pilote L. Statins and cancer risk. Am J Med 2008;121:302–9.
29. Kuoppala J, Lamminpaa A, Pukkala E. Statins and cancer: a systematic review and meta-analysis. Eur J Cancer 2008;44:2122–32.
30. Lubet RA, Boring D, Steele VE, Ruppert JM, Juliana MM, Grubbs CJ. Lack of efficacy of the statins atorvastatin and lovastatin in rodent mammary carcinogenesis. Cancer Prev Res 2009;2:161–7.
31. Bhuket TP, Higgins PD. Drug insight: statins and gastrointestinal cancer. Nat Clin Pract Gastroenterol Hepatol 2006;3:552–62.
32. Moorman PG, Hamilton RJ. Statins and cancer risk: what do we know and where do we go from here? Epidemiology 2007;18:194–6.
33. Saito Y, Yamada N, Teramoto T, et al. A randomized, double-blind trial comparing the efficacy and safety of pitavastatin versus pravastatin in patients with primary hypercholesterolemia. Atherosclerosis 2002;162:373–9.
34. Neuvonen PJ, Niemi M, Backman JT. Drug interactions with lipid-lowering drugs: mechanisms and clinical relevance. Clin Pharmacol Ther 2006;80: 565–81.
35. Sakagami T, Dixon M, O'Rourke J, et al. Atrophic gastric changes in both *Helicobacter felis* and *Helicobacter pylori* infected mice are host dependent and separate from antral gastritis. Gut 1996;39: 639–48.
36. Miyamoto S, Yasui Y, Kim M, et al. A novel rasH2 mouse carcinogenesis model that is highly susceptible to 4-NQO-induced tongue and esophageal carcinogenesis is useful for preclinical chemoprevention studies. Carcinogenesis 2008;29:418–26.
37. Cao X, Tsukamoto T, Nozaki K, et al. Severity of gastritis determines glandular stomach carcinogenesis in *Helicobacter pylori*-infected Mongolian gerbils. Cancer Sci 2007;98:478–83.
38. Pasceri V, Cammarota G, Patti G, et al. Association of virulent *Helicobacter pylori* strains with ischemic heart disease. Circulation 1998;97:1675–9.
39. Laurila A, Bloigu A, Nayha S, Hassi J, Leinonen M, Saikku P. Association of *Helicobacter pylori* infection with elevated serum lipids. Atherosclerosis 1999;142:207–10.
40. Kucukazman M, Yavuz B, Sacikara M, et al. The relationship between updated Sydney System score and LDL cholesterol levels in patients infected with *Helicobacter pylori*. Dig Dis Sci 2009; 54:604–7.
41. Takashima T, Adachi K, Kawamura A, et al. Cardiovascular risk factors in subjects with *Helicobacter pylori* infection. Helicobacter 2002;7:86–90.
42. Scragg RK, Fraser A, Metcalf PA. *Helicobacter pylori* seropositivity and cardiovascular risk factors in a multicultural workforce. J Epidemiol Community Health 1996;50:578–9.
43. Hoffmeister A, Rothenbacher D, Bode G, et al. Current infection with *Helicobacter pylori*, but not seropositivity to *Chlamydia pneumoniae* or cytomegalovirus, is associated with an atherogenic, modified lipid profile. Arterioscler Thromb Vasc Biol 2001;21:427–32.
44. Habara K, Hamada Y, Yamada M, et al. Pitavastatin up-regulates the induction of iNOS through enhanced stabilization of its mRNA in pro-inflammatory cytokine-stimulated hepatocytes. Nitric Oxide 2008;18:19–27.

Association of visceral fat accumulation and plasma adiponectin with rectal dysplastic aberrant crypt foci in a clinical population

Hirokazu Takahashi,[1,5] Tetsuji Takayama,[2] KyokoYoneda,[1] Hiroki Endo,[1] Hiroshi Iida,[1] Michiko Sugiyama,[1] Koji Fujita,[1] Masato Yoneda,[1] Masahiko Inamori,[1] Yasunobu Abe,[1] Satoru Saito,[1] Koichiro Wada,[3] Hitoshi Nakagama[4] and Atsushi Nakajima[1]

[1]Gastroenterology Division, Yokohama City University Graduate School of Medicine, Yokohama, Kanagawa 236-0004; [2]Gastroenterology Division, University of Tokushima Faculty of Medicine, Tokushima 770-8503; [3]Department of Pharmacology, School of Dentistry, Osaka University, Osaka 565-0871; [4]Biochemistry Division, National Cancer Center Research Institute, Tokyo 104-0045, Japan

(Received June 21, 2008/Revised August 31, 2008/Accepted September 5, 2008/Online publication October 23, 2008)

The association between obesity and the risk of colorectal cancer (CRC) cannot be easily evaluated because CRC itself is associated with a gradual loss of bodyweight. Aberrant crypt foci (ACF) can be classified as dysplastic ACF or non-dysplastic ACF by magnifying colonoscopy, and dysplastic ACF are thought to be a biomarker of CRC. Ninety-four participants who underwent colonoscopy at Yokohama City University Hospital, Japan, were enrolled in the current study. We detected 557 ACF, including 67 dysplastic ACF (12.0%). Univariate regression analysis was conducted to determine correlations between the number of dysplastic ACF and various potential risk factors, including patient age, waist circumference, body mass index, visceral fat area (VFA), and plasma adiponectin level. The results of multiple regression analysis revealed that the number of dysplastic ACF correlated with age (correlation coefficient $r = 0.212$, $P = 0.0383$) and plasma adiponectin level ($r = -0.201$, $P = 0.0371$), even after adjustments for sex, waist circumference, body mass index, and VFA. Our univariate correlation analysis data showed a significant correlation with the number of dysplastic ACF with VFA ($r = 0.238$, $P = 0.0209$), no correlation with subcutaneous fat area, and an inverse correlation with the plasma level of adiponectin ($r = -0.258$, $P = 0.0118$). Thus, our results suggest that aging and visceral fat accumulation could correlate moderately with colorectal carcinogenesis. The novelty of our study lies in the finding that visceral fat accumulation and a low plasma adiponectin level may promote colorectal carcinogenesis; therefore, these obesity-related parameters may serve as novel targets for CRC prevention. (*Cancer Sci* 2009; 100: 29–32)

Obesity and its associated visceral fat accumulation have been reported to be linked to an elevated risk of cardiovascular disease, diabetes mellitus, and mortality, and these complications are rapidly becoming significant problems.[1,2] Visceral adipose tissue is not only fat storage tissue, but also a metabolically active organ secreting many adipocytokines, such as adiponectin.[3] Obesity is reportedly an important risk factor for CRC.[4] CRC has high mortality and morbidity rates, and its prevalence has been increasing.[5,6] The precise risk factors for CRC remain unclear, although a family history and several dietary and lifestyle factors have been proposed to be involved.[7]

The association between obesity and the risk of CRC cannot be easily evaluated because of the confounding effect of bodyweight loss with CRC. Therefore, we sought to identify a biomarker for risk assessment and monitoring of CRC. ACF, which were first discovered in mice treated with azoxymethane,[8] have been clearly shown to be precursor lesions of CRC, and are now established as a biomarker of the risk of CRC in azoxymethane-treated mice and rats.[9] In humans, ACF can be classified as dysplastic or non-dysplastic through the use of magnifying colonoscopy.[10] ACF have not been firmly established to be precursors of CRC; however, dysplastic ACF could possibly serve as a biomarker of the risk of CRC. Previous studies have reported that individuals with CRC have more ACF than those without CRC, therefore dysplastic ACF represent potential clinical precursors of CRC and colorectal adenoma.[11–14] Recently, an association was suggested to exist between obesity and the risk of CRC.[15,16] However, the relationship between obesity and ACF remains unclear. Therefore, the current study in a clinical population aimed to investigate the relationship between various obesity-associated parameters and rectal dysplastic ACF.

Patients and Methods

Study population. We prospectively evaluated 94 subjects recruited from the population of healthy individuals who underwent colonoscopy at Yokohama City University Hospital, Japan. The exclusion criteria included: presence of contraindications to colonoscopy; current or past non-steroidal anti-inflammatory drug use including aspirin; family history of CRC; or history of adenoma, carcinoma, familial adenomatous polyposis, inflammatory bowel disease, or radiation colitis. Subjects with a history of colectomy, gastrectomy, or colorectal polypectomy, and those treated with daily insulin self-injection or sulfonylurea for diabetes mellitus, were also excluded. In order to investigate the influence of obesity on colorectal carcinogenesis, patients with colorectal adenoma or carcinoma at the time of colonoscopy were also excluded from the study. Written informed consent was obtained from all subjects prior to their participation. The study protocol was approved by the Yokohama City University Hospital Ethics Committee.

Collection and analysis of blood samples for adiponectin level. Blood samples were obtained in the morning on the day of colonoscopy after overnight fasting. Plasma adiponectin levels were measured by enzyme-linked immunosorbent assay of the total forms of human adiponectin (SRL Co., Tokyo, Japan).

Magnifying colonoscopy for identification of ACF. Participants' bowel preparation for the colonoscopy was carried out using

[5]To whom correspondence should be addressed.
E-mail: hirokazu@med.yokohama-cu.ac.jp
Abbreviations: ACF, aberrant crypt foci; BMI, body mass index; CRC, colorectal cancer; CT, computed tomography; SFA, subcutaneous fat area; TFA, total fat area; VFA, visceral fat area.

doi: 10.1111/j.1349-7006.2008.00994.x

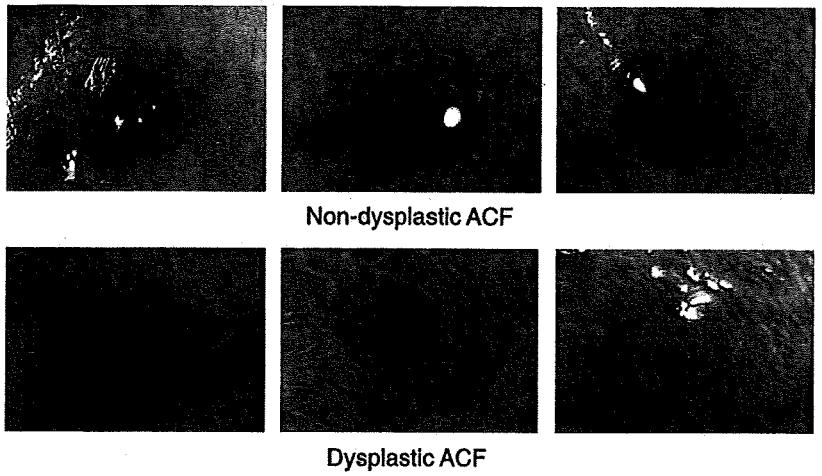

Fig. 1. Typical features of non-dysplastic and dysplastic aberrant crypt foci (ACF) on magnifying colonoscopy after methylene blue staining.

polyethylene glycol solution. A Fujinon EC-490ZW5/M colonoscope was used for the magnifying colonoscopy (Fujinon Toshiba ES Systems, Tokyo, Japan). Total colonoscopy was carried out before imaging of rectal ACF. Subsequently, 0.25% methylene blue was applied to the mucosa with a spray catheter. Aberrant crypts were distinguished from normal crypts by their deeper staining and larger diameter, and the number of ACF in the rectum was counted. This counting was conducted in the lower rectal region, extending from the middle Houston valve to the dentate line, based on the results of a previous study.[10] All ACF were recorded photographically and evaluated by two independent observers who were unaware of the subjects' clinical histories.

Criteria used for endoscopic diagnosis. ACF were defined as lesions in which the crypts were more darkly stained with methylene blue than normal crypts and had larger diameters, often with oval or slit-like lumens and a thicker epithelial lining.[17–20] Dysplastic ACF were defined as crypts in which each lumen was compressed or not distinct, with an epithelial lining that was much thicker than that of normal surrounding crypts. Non-dysplastic ACF were classified as hyperplastic or non-hyperplastic.[10]

Measurement of VFA and SFA. BMI was calculated using the following equation: bodyweight (kg)/(height [m]^2). Intra-abdominal adipose tissue was assessed, as described previously by measuring the VFA, SFA, TFA, and waist circumference from CT images at the level of the umbilicus.[4,10] All CT scans were carried out with the subjects in the supine position. The borders of the intra-abdominal cavity were outlined on the CT images, and the VFA was quantified using Fat Scan software (N2 System Corporation, Kobe, Japan).

Statistical analysis. We examined the associations between the risk factors for CRC and the number of dysplastic ACF. All data were expressed as mean ± SD, unless otherwise indicated. The relationships between the number of dysplastic ACF and relevant covariates were examined by univariate regression analysis, and standardized correlation coefficients were determined using Stat View software (SAS Institute, Cary, NC, USA). Multiple regression analysis was carried out to assess the relationship between the number of dysplastic ACF and potentially associated variables, and to determine the standardized correlation coefficients. The dependent variable was the number of dysplastic ACF, and the independent variables were age, sex, VFA, and plasma adiponectin level. Waist circumference and BMI were excluded from this analysis because these factors have a high correlation with VFA. P-values < 0.05 were considered to denote statistical significance.

Results

Colonoscopic features of ACF. A total of 557 ACF, including 67 dysplastic ACF, were counted by magnifying colonoscopy in the 94 patients. The aberrant crypts were larger, thicker, and more darkly stained than the normal crypts. Dysplastic ACF and non-dysplastic ACF accounted for 12.0% (67 of 557) and 88.0% (490 of 557) of the total, respectively. The number of subjects with dysplastic ACF was 34, and the number with non-dysplastic ACF was 76. In the lesions detected by magnifying colonoscopy, the size (i.e. median number of crypts ± SD) per ACF was 15.1 ± 10.4 and per dysplastic ACF was 8.5 ± 11.8. The average number of composition crypts per ACF was 93.2 ± 124.3 and per dysplastic ACF was 16.3 ± 26.2. In the 94 patients, the mean total number of ACF (non-dysplastic and dysplastic) per patient was 5.92 ± 6.50, and the mean number of dysplastic ACF per patient was 0.71 ± 1.16. The typical colonoscopic features of dysplastic and non-dysplastic ACF are shown in Figure 1.

Patient characteristics. The clinical characteristics of the study participants are shown in Table 1. The mean age was 65.1 ± 10.8 years, and there were 48 men and 46 women. The mean waist circumference, BMI, TFA, VFA, SFA, and plasma adiponectin level were 86.3 ± 10.0 cm, 23.3 ± 3.1 kg/m^2, 200.8 ± 91.4 cm^2, 83.9 ± 50.1 cm^2, 116.7 ± 60.4 cm^2, and 11.0 ± 5.6 μg/mL, respectively.

Univariate regression analysis: Correlations between risk factors for CRC and the number of dysplastic ACF. Age correlated significantly with the number of dysplastic ACF, as shown in Table 2 ($r = 0.232$, $P = 0.0242$). Sex showed no correlation with the number of dysplastic ACF. All of the obesity parameters, except SFA ($r = -0.001$, $P = 0.9979$), correlated significantly with the number of dysplastic ACF, as follows: waist circumference ($r = 0.225$, $P = 0.0293$), BMI ($r = 0.307$, $P = 0.0325$), and VFA ($r = 0.238$, $P = 0.0209$). The plasma level of adiponectin showed a significant inverse correlation with the number of dysplastic ACF ($r = -0.258$, $P = 0.0118$). Age was the only parameter that correlated significantly with the number of non-dysplastic ACF ($r = 0.218$, $P = 0.0336$), which were much more abundant than dysplastic ACF in the study subjects.

Multiple regression analysis: Correlations between risk factors for CRC and the number of dysplastic ACF. The results of the multiple regression analysis are shown in Table 3. After adjustments for sex, waist circumference, BMI, and VFA, the parameters of age and plasma adiponectin level still correlated significantly with the number of dysplastic ACF ($P = 0.0383$ and $P = 0.0371$, respectively).

doi: 10.1111/j.1349-7006.2008.00994.x

Table 1. Clinical characteristics of study participants

Characteristic	Overall	Subjects with non-dysplastic ACF	Subjects with dysplastic ACF
Number	94	76	34
Age (years)	65.1 ± 10.8	66.3 ± 10.1	66.2 ± 8.1
Sex (male : female)	48:46	43:33	21:13
Waist circumference (cm)	86.3 ± 10.0	86.0 ± 10.5	88.4 ± 11.2
Body mass index (kg/m^2)	23.3 ± 3.1	23.3 ± 3.2	24.2 ± 3.0
Total fat area (cm^2)	200.8 ± 91.4	199.5 ± 95.7	222.0 ± 96.0
Visceral fat area (cm^2)	83.9 ± 50.1	86.3 ± 51.6	103.6 ± 52.6
Ssubcutaneous fat area (cm^2)	116.7 ± 60.4	112.9 ± 60.8	117.8 ± 58.4
Plasma adiponectin (μg/mL)	11.0 ± 5.6	11.3 ± 5.8	9.4 ± 4.3

Data are expressed as mean ± SD. ACF, aberrant crypt foci.

Table 2. Univariate correlation analysis: Correlations between the number of non-dysplastic or dysplastic aberrant crypt foci (ACF) and the risk factors for colorectal cancer

Risk factor	Non-dysplastic ACF		Dysplastic ACF	
	r	*P*	*r*	*P*
Age	0.218	0.0336*	0.232	0.0242*
Sex	0.109	0.2928	0.087	0.4069
Waist circumference	0.076	0.4651	0.225	0.0293*
Body mass index	0.169	0.1011	0.307	0.0325*
Total fat area	0.126	0.2257	0.135	0.1941
Visceral fat area	0.137	0.1868	0.238	0.0209*
Subcutaneous fat area	0.078	0.4560	−0.001	0.9979
Plasma adiponectin	−0.019	0.8538	−0.258	0.0118*

Age, waist circumference, body mass index, visceral fat area, and plasma adiponectin level correlated with the number of dysplastic ACF.
*$P < 0.05$.

Table 3. Multiple regression analysis: Correlations between the number of dysplastic aberrant crypt foci and the risk factors for colorectal cancer

Risk factor	Correlation coefficient	*P*
Age	0.212	0.0383*
Sex	0.038	0.7141
Waist circumference	−0.152	0.4508
Body mass index	0.249	0.1618
Visceral fat area	0.089	0.5807
Plasma adiponectin	−0.201	0.0371*

R^2 for the entire model = 0.368.
After adjustments for sex, waist circumference, body mass index, and visceral fat area, the parameters of age and plasma adiponectin level still correlated with the number of dysplastic aberrant crypt foci.
*$P < 0.05$.

Discussion

In the present study a total of 557 ACF were counted in the 94 patients, and we demonstrated a significant correlation between the number of dysplastic ACF and the VFA, and a significant inverse correlation between the number of dysplastic ACF and the plasma adiponectin level. Age was also associated with the number of ACF, that is, the number of dysplastic and non-dysplastic ACF increased with age. CRC is thought to progress through several morphological stages, from the formation of polyps to the onset of malignant change.[21] Genetic alterations, including mutations in the *K-ras*, *p53*, and *APC* genes, have been reported to be associated with the disease progression.[22] The *K-ras* mutation has also been reported in human ACF.[23] Therefore, the increased risk of ACF formation with age may be influenced mainly by these genetic alterations. Sex showed no correlation with the number of dysplastic ACF in the present study; however, the incidence of CRC is lower in women than in men.[24,25] It has been suggested that the initiation of dysplastic ACF is comparable in men and women, but thereafter tumor progression differs because visceral fat accumulation is higher in men than woman. This visceral fat accumulation may affect tumor progression.

Waist circumference has often been suggested to be associated with VFA. Consistent with this suggestion, our data showed that both waist circumference and VFA were associated with the number of dysplastic ACF. Recent reports have suggested that obesity may be associated with a high risk of CRC.[4] Several studies have shown that increased BMI is associated with an increased risk of CRC.[26] The importance of the size of ACF has been reported,[27] and the correlation between size, measured as the median number of crypts per both non-dysplastic ACF and dysplastic ACF, and risk factors was analyzed. The correlation between the median number of crypts per ACF and any risk factors had almost the same result as the number of ACF (data not shown). Our data showed a direct correlation between the VFA and the number of dysplastic ACF, and an inverse correlation between the plasma adiponectin level and the number of dysplastic ACF (Table 2). A previous study showed that the *K-ras* gene was mutated in 50–60% of patients with dysplastic ACF,[10] thus genetic alterations were already underway. Visceral fat correlated with dysplastic ACF in the current study, and another study showed that increased visceral adiposity was a significant predictor of lower rates of disease-free survival in patients with resectable colorectal cancer,[28] suggesting that visceral fat plays an important role in colorectal carcinogenesis and progression. Visceral fat tissue is known to be an endocrine organ that secretes adiponectin, which has an inverse relationship with obesity and visceral fat.[29] We carried out multiple regression analysis to assess whether plasma adiponectin may be a risk factor for dysplastic ACF growth, independent of the effects of obesity. If dysplastic ACF are a biomarker of the risk of colorectal adenoma and CRC, then some factors associated with the risk of CRC may also influence the number of dysplastic ACF. Very little is known about the factors that initiate or promote the growth of dysplastic ACF in humans. Our results suggest that plasma adiponectin levels are inversely associated with the number of ACF, and that visceral fat may be associated directly with ACF and thus could be a risk factor for the early stage of colorectal carcinogenesis.

There are many reports on the existence of relationships between the risk of CRC and exercise, energy use, glycemic index, and food choices and dietary constituents.[30–32] These factors affect each other, therefore it is difficult to evaluate the relationship between any one factor and the risk of CRC. Obesity

is thought to result from many of these factors. It is also thought that aging, visceral fat, and adiponectin are important in CRC carcinogenesis. Further investigation is needed to elucidate the mechanisms that affect these relationships and the impact on the development of CRC.

The novelty of our study lies in our use of dysplastic ACF as a biomarker for risk of CRC to show that visceral fat accumulation and low plasma adiponectin level may affect colorectal carcinogenesis. Further studies should be conducted to clarify the role that visceral fat accumulation and reduced plasma adiponectin play in dysplastic ACF growth and whether these obesity-related parameters may serve as novel targets for CRC prevention.

Acknowledgments

We thank Machiko Hiraga for her technical assistance. This work was supported in part by a Grant-in-Aid for research on the Third Term Comprehensive Control Research for Cancer from the Ministry of Health, Labour, and Welfare, Japan to A.N., a grant from the National Institute of Biomedical Innovation to A.N., a grant from the Ministry of Education, Culture, Sports, Science, and Technology, Japan (KIBAN-B) to A.N., a grant from the Ministry of Education, Culture, Sports, Science, and Technology, Japan (WAKATE-B) to H.T., a research grant from the Princess Takamatsu Cancer Research Fund to A.N., and a grant for the 2007 Strategic Research Project (no. K19041) of Yokohama City University, Japan to H.T. and A.N.

References

1 Fujioka S, Matsuzawa Y, Tokunaga K *et al.* Contribution of intra-abdominal fat accumulation to the impairment of glucose and lipid metabolism in human obesity. *Metabolism* 1987; **36**: 54–9.
2 Kissebah AH, Vydelingum N, Murray R *et al.* Relation of body fat distribution to metabolic complications of obesity. *J Clin Endocrinol Metab* 1982; **54**: 254–60.
3 Park KG, Park KS, Kim MJ *et al.* Relationship between serum adiponectin and leptin concentrations and body fat distribution. *Diabetes Res Clin Pract* 2004; **63**: 135–42.
4 Giovannucci E, Aasherio A, Rimm EB *et al.* Physical activity, obesity, and risk for colon cancer and adenoma in men. *Ann Intern Med* 1995; **122**: 327–34.
5 Anderson WF, Umar A, Brawley OW. Colorectal carcinoma in black and white race. *Cancer Metastasis Rev* 2003; **22**: 67–82.
6 Rougier P, Mitry E. Epidemiology, treatment and chemoprevention in colorectal cancer. *Ann Oncol* 2003: **14**: ii3–5.
7 Garland C, Shekelle RB, Barrett-Connor E *et al.* Dietary vitamin D and calcium and risk of colorectal cancer: a 19-year prospective study in men. *Lancet* 1985; **1**: 307–9.
8 Bird RP. Observation and quantification of aberrant crypts in the murine colon treated with a colon carcinogen: preliminary findings. *Cancer Lett* 1987; **37**: 147–51.
9 Pretlow TP, O'Riordan MA, Somich GA *et al.* Aberrant crypts correlate with tumor incidence in F344 rats treated with azoxymethane and phytate. *Carcinogenesis* 1992; **13**: 1509–12.
10 Takayama T, Katsuki S, Takahashi Y *et al.* Aberrant crypt foci of the colon as precursors of adenoma and cancer. *N Engl J Med* 1998; **339**: 1277–84.
11 Nascimbeni R, Villanacci V, Mariani PP *et al.* Aberrant crypt foci in the human colon: frequency and histologic patterns in patients with colorectal cancer or diverticular disease. *Am J Surg Pathol* 1999; **23**: 1256–63.
12 Shpitz B, Bomstein Y, Mekori Y *et al.* Aberrant crypt foci in human colons: distribution and histomorphologic characteristics. *Hum Pathol* 1998; **29**: 469–75.
13 Adler DG, Gostout CJ, Sorbi D *et al.* Endoscopic identification and quantification of aberrant crypt foci in the human colon. *Gastrointest Endosc* 2002; **56**: 657–62.
14 Nucci MR, Robinson CR, Longo P *et al.* Phenotypic and genotypic characteristics of aberrant crypt foci in human colorectal mucosa. *Hum Pathol* 1997; **28**: 1396–407.
15 Gunter MJ, Leitzmann MF. Obesity and colorectal cancer: epidemiology, mechanisms and candidate genes. *J Nutr Biochem* 2006; **17**: 145–56.
16 Otake S, Takeda H, Suzuki Y *et al.* Association of visceral fat accumulation and plasma adiponectin with colorectal adenoma: evidence for participation of insulin resistance. *Clin Cancer Res* 2005; **11**: 3642–6.
17 Roncucci L, Stamp D, Medline A *et al.* Identification and quantification of aberrant crypt foci and microadenomas in the human colon. *Hum Pathol* 1991; **22**: 287–94.
18 Roncucci L, Medline A, Bruce WR. Classification of aberrant crypt foci and microadenomas in human colon. *Cancer Epidemiol Biomarkers Prev* 1991; **1**: 57–60.
19 Pretlow TP, Barrow BJ, Ashton WS *et al.* Aberrant crypts: putative preneoplastic foci in human colonic mucosa. *Cancer Res* 1991; **51**: 1564–7.
20 Pretlow TP, O'Riordan MA, Pretlow TG *et al.* Aberrant crypts in human colonic mucosa: putative preneoplastic lesions. *J Cell Biochem Suppl* 1992; **16**: 55–62.
21 Kinzler KW, Vogelstein B. Lessons from hereditary colorectal cancer. *Cell* 1996; **87**: 159–70.
22 Fearon ER, Vogelstein B. A genetic model for colorectal tumorigenesis. *Cell* 1990; **61**: 759–67.
23 Yuan P, Sun MH, Zhang JS *et al.* APC and K-ras gene mutation in aberrant crypt foci of human colon. *World J Gastroenterol* 2001; **7**: 352–6.
24 Gao RN, Neutel CI, Wai E. Gender differences in colorectal cancer incidence, mortality, hospitalizations and surgical procedures in Canada. *J Public Health* 2008; **30**: 194–201.
25 de Kok IM, Wong CS, Chia KS *et al.* Gender differences in the trend of colorectal cancer incidence in Singapore, 1968–2002. *Int J Colorectal Dis* 2008; **23**: 461–7.
26 Graham S, Marshall J, Haughey B *et al.* Dietary epidemiology of cancer of the colon in western New York. *Am J Epidemiol* 1988; **128**: 490–503.
27 Rudolph RE, Dominitz JA, Lampe JW *et al.* Risk factors for colorectal cancer in relation to number and size of aberrant crypt foci in humans. *Cancer Epidemiol Biomarkers Prev* 2005; **14**: 605–8.
28 Moon HG, Ju YT, Jeong CY *et al.* Visceral obesity may affect oncologic outcome in patients with colorectal cancer. *Ann Surg Oncol* 2008; **15**: 1918–22.
29 Arita Y, Kihara S, Ouchi N *et al.* Paradoxical decrease of an adipose-specific protein, adiponectin, in obesity. *Biochem Biophys Res Commun* 1999; **257**: 79–83.
30 Gerhardsson M, Floderus B, Norell SE. Physical activity and colon cancer risk. *Int J Epidemiol* 1988; **17**: 743–6.
31 Slattery ML, Benson J, Berry TD *et al.* Dietary sugar and colon cancer. *Cancer Epidemiol Biomarkers Prev* 1997; **6**: 677–85.
32 Reedy J, Haines PS, Steckler A *et al.* Qualitative comparison of dietary choices and dietary supplement use among older adults with and without a history of colorectal cancer. *J Nutr Educ Behav* 2005; **37**: 252–8.

doi: 10.1111/j.1349-7006.2008.00994.x

J Gastroenterol (2009) 44:964–975
DOI 10.1007/s00535-009-0089-8

ORIGINAL ARTICLE—LIVER, PANCREAS, AND BILIARY TRACT

Suppressive effect of sulindac on branch duct-intraductal papillary mucinous neoplasms

Tsuyoshi Hayashi · Hirotoshi Ishiwatari · Hideyuki Ihara · Yutaka Kawano · Koichi Takada · Koji Miyanishi · Masayoshi Kobune · Rishu Takimoto · Tomoko Sonoda · Tetsuji Takayama · Junji Kato · Yoshiro Niitsu

Received: 4 February 2009 / Accepted: 29 April 2009 / Published online: 18 June 2009

Abstract
Backgound When considering surgery for branch duct-intraductal papillary mucinous neoplasms (BD-IPMNs) with suspected malignancy, it should be recognized that these lesions are frequently multifocal and are usually found in elderly patients with potential comorbidities that could affect the outcome of surgery. Clinical trials of chemoprevention have been conducted for a wide variety of malignancies.
Methods Twenty-two BD-IPMN patients participated in the trial at our institution from June 2004 to January 2007. Ten of the 22 patients who rejected surgical therapy although their lesions or clinical symptoms met the criteria for surgical resection of the International Association of Pancreatology guidelines were assigned to the treatment group. Sulindac (150 mg twice daily) and omeprazole (20 mg once daily) were administered to these patients for 18 months. The remaining 12 patients comprised the control group. Branch duct diameter and mural nodule heights were monitored by either magnetic resonance cholangiopancreatography (MRCP) or computed tomography (CT) and by endoscopic ultrasonography (EUS).
Results Both branch duct diameter and mural nodule height of BD-IPMNs in the treatment group were significantly reduced, while those in the control group were unchanged. Immunohistochemical staining for cyclooxygenase-1 and -2 was negative in hyperplasia, adenoma and carcinoma portions of resected pancreatic specimens but was clearly positive for glutathione-*S*-transferase π (GST-π), suggesting that GST-π is a putative target molecule for sulindac.
Conclusions Although a larger scale randomized controlled study is needed in future, the present results suggest the promise of chemoprevention of carcinoma derived from BD-IPMNs by sulindac.

Keywords Intraductal papillary-mucinous neoplasm · Chemoprevention · Non-steroidal anti-inflammatory drugs · Glutathione-*S*-transferase π

Abbreviations

IAP	International Association of Pancreatology
BD-IPMNs	Branch duct intraductal papillary-mucinous neoplasm
MD-IPMN	Main duct intraductal papillary-mucinous neoplasm
ERP	Endoscopic retrograde pancreatography
CT	Computed tomography
MRCP	Magnetic resonance cholangiopancreatography
EUS	Endoscopic ultrasonography
NSAIDs	Non-steroidal anti-inflammatory drugs

T. Hayashi · H. Ishiwatari · H. Ihara · Y. Kawano · K. Takada · K. Miyanishi · M. Kobune · R. Takimoto · J. Kato
Fourth Department of Internal Medicine,
Sapporo Medical University School of Medicine,
Sapporo, Japan

T. Sonoda
Department of Public Health, Sapporo Medical University School of Medicine, Sapporo, Japan

T. Takayama
Department of Gastroenterology and Oncology,
Institute of Health Biosciences,
The University of Tokushima Graduate School,
Sapporo, Japan

Y. Niitsu (✉)
Department of Molecular Target Exploration,
Sapporo Medical University School of Medicine,
South-1, West-16 Chuo-ku Sapporo,
Hokkaido 060-8556, Japan
e-mail: niitsu@sapmed.ac.jp

COX-1 Cyclooxygenase-1
COX-2 Cyclooxygenase-2
GST-π Glutathione-*S*-transferase π

Introduction

Over the past 15 years, mostly due to developments in high-resolution abdominal imaging techniques, the number of patients found to have intraductal papillary mucinous neoplasms (IPMNs) has dramatically increased. IPMNs can be categorized into two groups based on a topographical difference: neoplasms arising from the main pancreatic duct (MD-IPMNs) and IPMNs involving only the secondary branch ducts (BD-IPMNs). Recent studies have revealed that these two types of IPMNs also differ with regard to biological behavior, such as invasiveness and expansion rate [1]. The prevalence of cancer among MD-IPMNs and BD-IPMNs ranges from 57–92% to 6–46%, respectively, indicating immediate surgical resection for the former lesion [2–5]. As to the therapeutic strategy for the latter lesion, the International Association of Pancreatology (IAP) suggests that patients with no symptoms, with a branch duct diameter of <30 mm, with no mural nodules and a main pancreatic duct diameter <6 mm can be followed with periodic imaging and that patients who develop any one of those four findings should undergo surgery [6]. However, when considering surgery for BD-IPMNs, it should be noted that the lesions are frequently multifocal, are usually found in elderly patients with potential comorbidities that can affect the outcome after surgery, and are associated with a high incidence of extra pancreatic malignancies.

Clinical trials of chemoprevention have been conducted for a wide variety of malignancies, including colorectal cancer, lung cancer, etc. [7–10]. Since chemoprevention is a more active approach than the simple watch and wait follow-up for non-operative BD-IPMNs and is considered to be suitable for avoiding the difficulties described above, in the present study, we attempted to treat patients with BD-IPMNs who had refused surgery with a non-steroidal anti-inflammatory drugs (NSAIDs), sulindac, which has been used to suppress the growth of pancreatic cancer cell line and to prevent the occurrence of pancreatic neoplasia [11–13].

Methods

Clinical trial of sulindac administration to patients with IPMNs

This clinical trial was approved by Institutional Review Board of Sapporo Medical University. Written informed consent was obtained from all enrolled subjects.

Forty patients were diagnosed to have BD-IPMNs, which were grape-like multilocular cysts with a communication to the main pancreatic duct, based on results of magnetic resonance cholangiopancreatography (MRCP) or computed tomography (CT) at our institution from June 2004 to January 2007. Of these, a total of 22 patients entered into the trial. Ten of these 22 patients had refused surgical therapy although their lesions or clinical symptoms met the criteria for surgical resection as defined by IAP guidelines and were assigned to the treatment group. They had no history of regular use of NSAIDs, active peptic ulcer, renal dysfunction or allergy to NSAIDs. Administration of sulindac (150 mg twice daily) to the treatment group was continued for 18 months. This dosage was chosen according to the previous chemopreventive studies for colorectal cancer [14, 15]. To prevent mucosal damage by sulindac, omeprazole (20 mg once daily) was also administered. The remaining 12 patients included 11 patients whose lesions did not meet the criteria for surgical resection and one patient (case 11) who had a history of aspirin asthma and refused surgery, although surgical resection was indicated for her lesion. These 12 patients comprised the control group.

Branch duct diameter and main pancreatic duct diameter were monitored by either MRCP or CT twice (at 6 and 18 months) during the observation period. The height of mural nodules was measured by endoscopic ultrasonography (EUS).

Immunohistochemistry

To explore the putative target molecule for sulindac, we performed immunohistochemical studies of cyclooxygenase-1 (COX-1), cyclooxygenase-2 (COX-2) and glutathione-*S*-transferase π (GST-π) using eight specimens of BD-IPMNs that had been resected at our institution between 2000 and 2007. None were from the treatment or control group. In all cases, not only high-grade lesions but also low-grade lesions spreading to the surrounding areas were evaluated. Lesions corresponding to mucinous hyperplasia according to Soldini et al. [16] were defined as hyperplasia, lesions with low to moderate grade dysplasia according to World Health Organization classification [17, 18] as adenoma and lesions with high grade dysplasia and those with invasive carcinoma, according to World Health Organization classification as carcinoma.

Antigen retrieval was performed in Target Retrieval Solution High pH (DAKO, Carpentaria, CA, USA) heated at 100°C in an autoclave for 5 min. Immunohistochemical staining of COX-1 and COX-2 was performed by the LSAB method using an anti-COX-1 polyclonal antibody (Santa Cruz Biotechnology Inc, Santa Cruz, CA, USA) and anti-COX-2 polyclonal antibody (Santa Cruz Biotechnology

Inc), respectively, and LSAB + System-HRP (DAKO). Immunohistochemical staining of GST-π was performed by the dextran polymer method using an anti-GST-π polyclonal antibody (MBL, Nagoya, Japan) and Envision Kit (DAKO), followed by coloring with 3,3′-diaminobenzidine tetrahydrochloride (DAB) (Wako, Osaka, Japan) and nuclear staining with Gill's hematoxylin solution (Wako). Staining intensity and width of staining area under three microscopic fields with a magnification of 200 × were graded according to the method of Gong et al. [19]. Score of intensity and score of area were multiplied and the resultant number was expressed as shown in Fig. 7.

Statistical analysis

Statistical analyses were performed using the Fisher exact test for gender and multiplicity of lesions and Mann–Whitney U test for age, branch duct diameter, main pancreatic duct diameter and mural nodule height. Spearman's rank correlation coefficient was determined for the relation between the branch duct diameter and mural nodule height. Friedman's test and Wilcoxon signed-rank test were performed to determine changes during the observation period. Differences were considered significant at a P value of less than 0.05 in the above analysis. Wilcoxon signed-rank test was used for multiple comparisons of scores of immunohistochemical staining intensity, and the Bonferroni correction was applied.

Results

Demographics of patients

Demographics of patients and their BD-IPMN lesion on images are shown in Table 1. Although there were no differences in age ($P = 0.39$), gender ($P = 0.37$), multiplicity of lesions ($P = 0.59$), branch duct diameter ($P = 0.12$) and main pancreatic duct diameter ($P = 0.34$) between the treatment and control groups, mural nodule height differed significantly between the two groups ($P = 0.003$). Cases 1–10 comprised the treatment group and cases 11–22 the control group.

In case 1, two dilated branch ducts with diameters of 56 and 24 mm, respectively, were detected by MRCP. A mural nodule was associated with the latter duct. In cases 2, 3, and 4, branch duct diameter exceeded 30 mm and mural nodules were detected. Although the branch duct diameter in cases 5, 6, 8, 9, and 10 was within 30 mm, mural nodules were detected in each of these cases. Case 7 experienced continuous epigastric abdominal pain, which is one of the IAP criteria for surgical resection of the lesion. Thus all patients in the treatment group were recommended to undergo surgery according to IAP guidelines, but rejected the recommendation. Cases 8 and 10 transiently complained of lower abdominal pain, which was irrelevant to the pancreatic lesion.

In the control group, case 11 had a lesion with a branch duct diameter >30 mm, main pancreatic duct diameter >6 mm, and mural nodule, which undoubtedly met the criteria of surgical resection, but she rejected operation. This patient had a history of aspirin asthma and therefore was not eligible for treatment with sulindac. The remaining 11 patients in the control group had lesions that did not indicate surgical resection.

To evaluate the relation between branch duct diameter and mural nodule height as determined by either MRCP or CT and EUS, respectively, we conducted Spearman rank-order correlation coefficient analysis and found no statistically significant correlation ($r = 0.40$, $P = 0.067$).

Changes in branch duct diameter in the treatment group and control group during the 18-month observation period

In the treatment group, there was an apparent decrease in branch duct diameter during the period of treatment in cases 1, 2, 3, 4, 8, and 10, although regrowth of the diameter of the branch duct after 6 months was observed in Patient 2. On the other hand, in cases 5, 6, 7, and 9, the branch duct diameter was unchanged. However, when the Friedman test was applied to this treatment group as a whole, the decrease in branch duct diameter was statistically significant ($P = 0.000055$). In the control group, the branch duct diameter tended to increase although the increment was not statistically significant ($P = 0.12$). Of note, in case 16, the branch duct diameter transiently increased at month 6 and decreased at month 18, possibly reflecting a change in the balance between the rate of mucin production by the mural nodule and the drainage rate of mucin fluid from the branch duct (Fig. 1.).

Changes in diameter of the main pancreatic duct in the treatment and control groups during the 18-month observation period

There were no significant changes in the diameter of the main pancreatic duct in both the treatment and control groups, including case 11, whose MPD was apparently dilated (Fig. 2.).

Changes in mural nodule height in the treatment and control groups during the 18-month observation period

In the entire treatment group, with the exception of cases 4 and 7 who had no mural nodules, mural nodule height

Table 1 Demographics of patients and their BD-IPMN lesions on images

	Case number	Age	Gender	Number of lesions	Location of main lesion	Indication of resection (reason for not undergoing operation)	Symptom at the diagnosis	Imaging modalities	Branch duct diameter (mm)	Main pancreatic duct diameter (mm)	Mural nodule height (mm)
Treatment group	1	55	M	2	Head	Yes (rejected)	Asymptomatic	MR + EUS	56 (24)[a]	5	0 (5)[a]
	2	78	M	1	Head	Yes (rejected)	Transient abdominal pain	CT + EUS	42	6	6
	3	74	F	1	Head	Yes (rejected)	Asymptomatic	MR + EUS	36	1	3
	4	65	M	1	Head	Yes (rejected)	Asymptomatic	MR + EUS	33	3	0
	5	70	M	3	Head	Yes (rejected)	Asymptomatic	MR + EUS	26	3	1
	6	47	M	1	Body	Yes (rejected)	Asymptomatic	CT + EUS	20	0	3
	7	61	F	1	Body	Yes (rejected)	Continuous abdominal pain	CT + EUS	17	3	0
	8	57	F	1	Head	Yes (rejected)	Transient abdominal pain	CT + EUS	17	2	7
	9	63	M	1	Tail	Yes (rejected)	Asymptomatic	MR + EUS	16	4	3
	10	57	F	Multiple	Head	Yes (rejected)	Asymptomatic	MR + EUS	13	2	4
Median		63.0							23.0	3.0	3.0
Control group	11	78	F	1	Body	Yes (asthma)	Asymptomatic	CT + EUS	40	15	7
	12	47	M	1	Head	No	Asymptomatic	MR + EUS	29	4	0
	13	86	F	2	Head	No	Asymptomatic	MR + EUS	23	0	0
	14	75	F	3	Head	No	Asymptomatic	MR + EUS	20	4	0
	15	62	M	1	Body	No	Asymptomatic	CT + EUS	19	0	0
	16	85	M	1	Body	No	Asymptomatic	MR + EUS	17	2	0
	17	62	F	1	Head	No	Asymptomatic	CT + EUS	17	0	0
	18	60	F	1	Body	No	Transient abdominal pain	MR + EUS	17	0	0
	19	57	F	Multiple	Tail	No	Asymptomatic	CT + EUS	15	2	0
	20	57	M	1	Head	No	Transient abdominal pain	MR + EUS	14	2	0
	21	72	F	2	Body	No	Asymptomatic	MR + EUS	11	4	0
	22	65	F	Multiple	Head	No	Asymptomatic	MR + EUS	10	3	0
Median		63.5							17.0	2.0	0

[a] Number in parentheses indicates branch duct diameter and mural nodule height of the smaller lesion

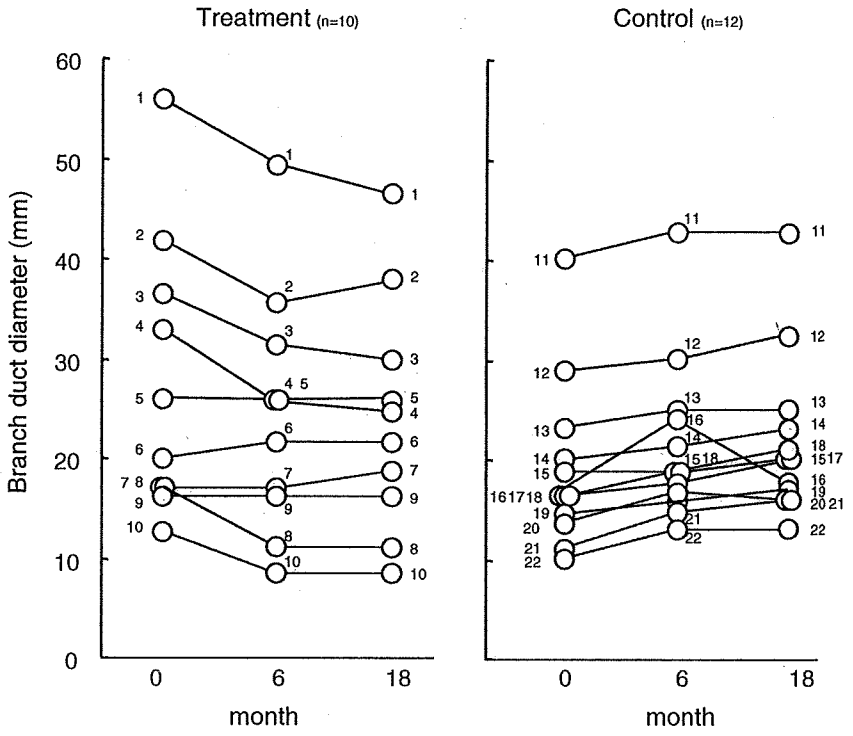

Fig. 1 Changes in branch duct diameter during the observation period. Number at each point (*circles*) represents case number. Friedman's test was used. Significant changes were observed in the treatment group ($P = 0.000055$) but not in the control group ($P = 0.12$)

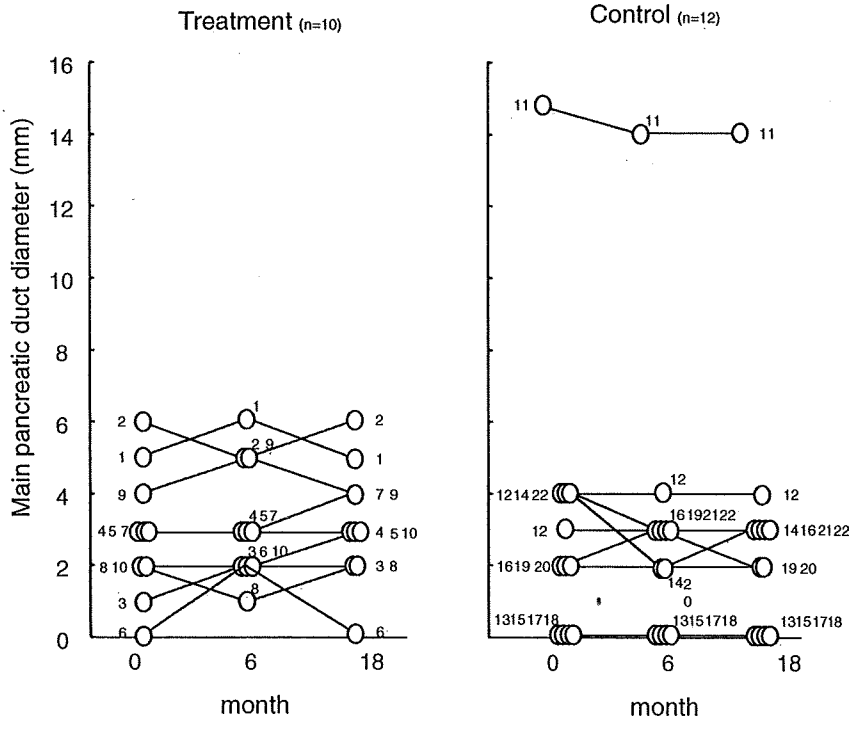

Fig. 2 Changes in diameter of the main pancreatic duct during the observation period. Number at each point (*circles*) represents case number. Friedman's test was used. Significant changes were not observed in either the treatment group ($P = 0.75$) or control group ($P = 0.66$)

decreased either by 6 or 18 months of treatment. The decrement was statistically significant by the Friedman test ($P = 0.001$). When mural nodule height was compared with branch duct diameter in each case, no correlation was observed. In cases 5, 6, and 9, who had no change in branch duct diameter, mural nodule height was clearly decreased.

In the control group, only one of 12 patients (case 11) had a detectable mural nodule. Monitoring of the lesion was performed in 8 of 12 patients which included case 11 because the other control group patients refused to undergo EUS. During 6 months of observation by EUS, mural nodule in case 11 clearly increased and only case 21 but not other cases developed a new mural nodule (Fig. 3).

Adverse effects

Among ten patients who received sulindac, none complained symptoms or suffered from apparent adverse effect related to sulindac.

Images of three representative cases (cases 1, 8, and 11)

Figures 4, 5, and 6 show impressive changes in lesions as observed by imaging modalities in three patients during the observation period.

Figure 4 shows an enlarged orifice of the ampulla of Vater (a), filling defect in the main pancreatic duct (white arrow, b), the communication of the dilated branch duct to the main pancreatic duct (white bracket, b), and grape-like multilocular cysts (white bracket, c) in case 1, which were all typical imaging features of BD-IPMNs. In this case, there were two dilated branch ducts, with diameters of 56 and 24 mm, respectively (Fig. 4c), and a nodule was present in the small branch duct. The maximum branch duct diameter decreased from 56 mm (large white bracket, Fig. 4c) to 49 mm (large white bracket, Fig. 4d) by 6 months and to 46 mm (large white bracket, Fig. 4e) by 18 months after initiation of the drug administration. The mural nodule height in the smaller branch duct was also reduced from 5 mm (white arrowhead, Fig. 4f) to 3 mm (white arrowhead, Fig. 4g) by 6 months.

Another patient (case 8) in the treatment group with a striking reduction in lesion size is shown in Fig. 5. Before the treatment, viscous fluid oozing from the ampulla of Vater (Fig. 5a), a dilated branch duct communicating to the main pancreatic duct (white bracket, Fig. 5b), and a cystic lesion in the pancreas (white bracket, Fig. 5c) were evident. Upon treatment, the diameter of the branch duct had reduced from 17 mm (white bracket, Fig. 5c) to 11 mm (white bracket, Fig. 5d) by 6 months, and remained at 11 mm (white bracket, Fig. 5e) at the 18th month. The height of the mural nodule in this case was also dramatically reduced from 7 mm (white arrowhead, Fig. 5f) to 4 mm (white arrowhead, Fig. 5g) by the 6 month of observation.

In contrast, the lesion clearly grew in size in one patient (case 11), the control group subject who rejected surgery despite meeting the criteria of the IAP and was not eligible for treatment with sulindac because of a history of allergy to NSAIDs. Figure 6 shows an enlarged orifice of Vater

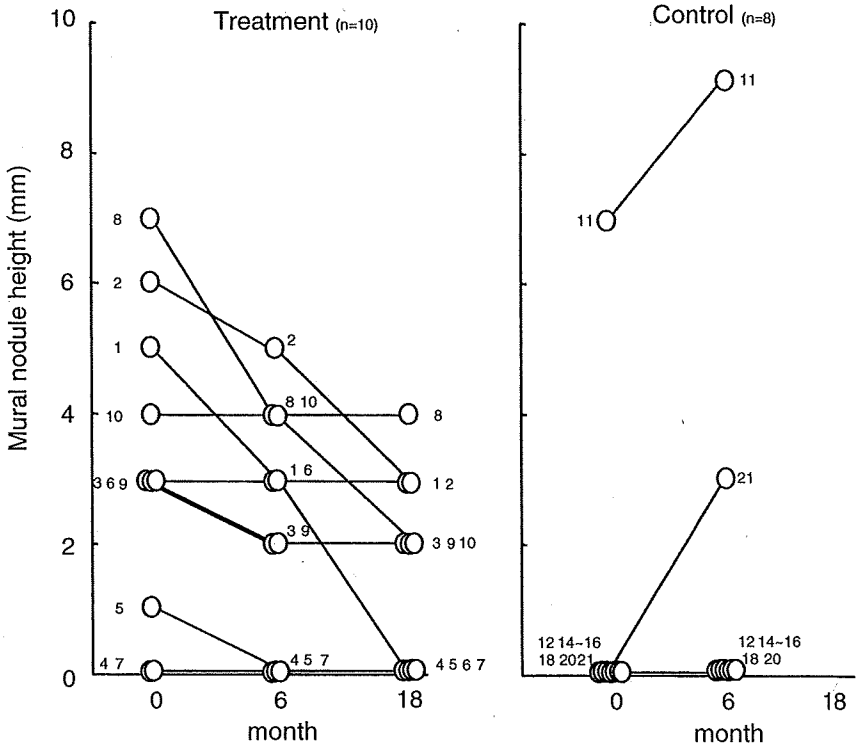

Fig. 3 Changes in mural nodule height during the observation period. Number at each point (*circles*) represents case number. Friedman's test was used. Significant changes were observed in the treatment group. ($P = 0.001$). Wilcoxon signed-rank test was performed. Significant changes were not observed in the control group ($P = 0.09$)

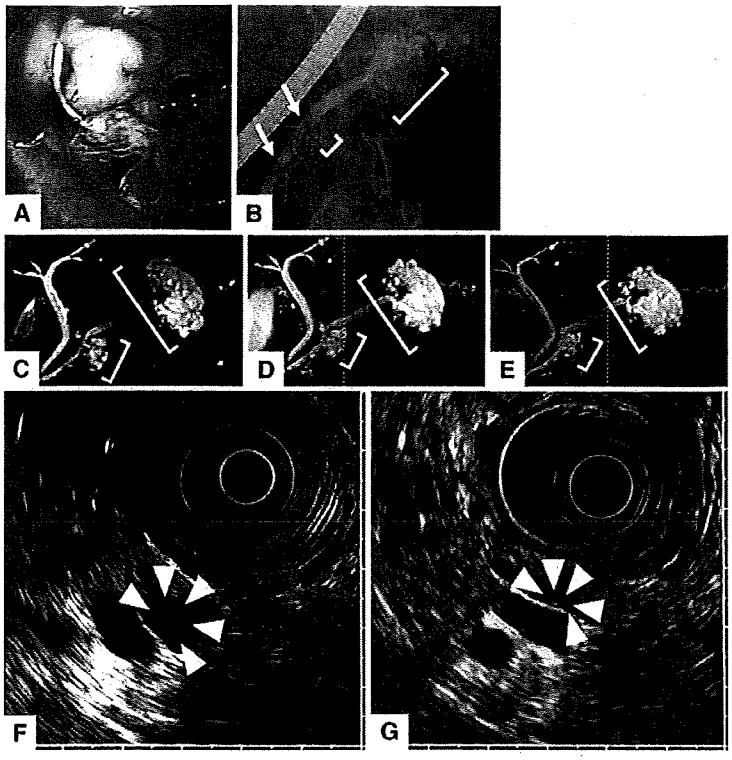

Fig. 4 Image findings in case 1. Duodenoscopic image of ampulla of Vater (**a**). ERP image of filling defect in moderately dilated main pancreatic duct and two dilated branch ducts (**b**). MRCP image of two dilated branch ducts and main pancreatic duct (**c** before drug administration, **d** 6 months after drug administration, **e**: 18 months after drug administration). EUS view of mural nodule in smaller dilated branch duct (**f** before drug administration, **g** 6 months after drug administration)

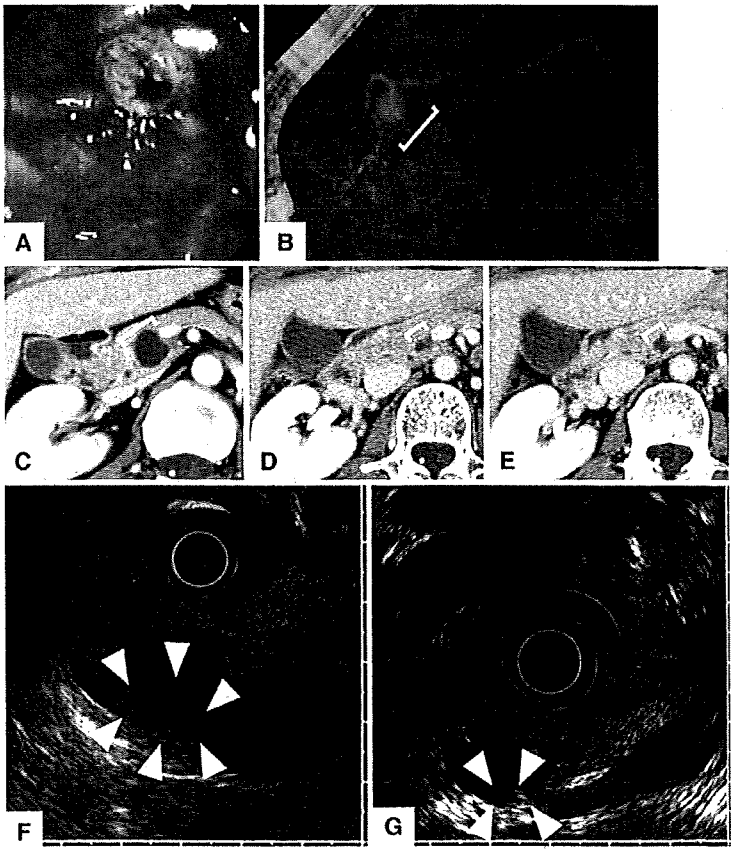

Fig. 5 Image findings in case 8. Duodenoscopic image of ampulla of Vater (**a**). ERP image of dilated branch duct communicating to main pancreatic duct (**b**). CT scans of cystic lesion of pancreas head (**c** before drug administration, **d** 6 months after drug administration, **e** 18 months after drug administration). EUS view of mural nodule in dilated branch duct (**f** before drug administration, **g** 6 months after drug administration)

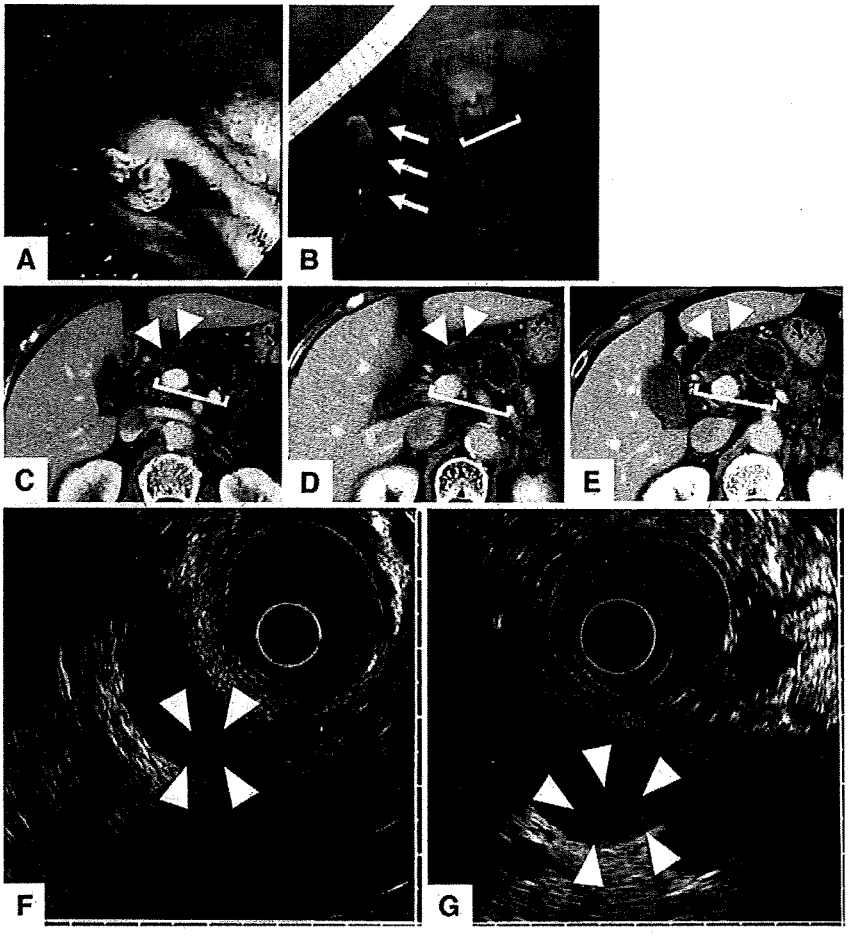

Fig. 6 Image findings in case 11. Duodenoscopic image of ampulla of Vater (**a**). ERP image of filling defect in moderately dilated main pancreatic duct and dilated branch duct (**b**). CT scans of multilocular cystic lesion of pancreas body (**c** before observation, **d** 6 months after observation, **e** 18 months after observation). EUS view of mural nodule in dilated branch duct (**f** before observation, **g** 6 months after observation)

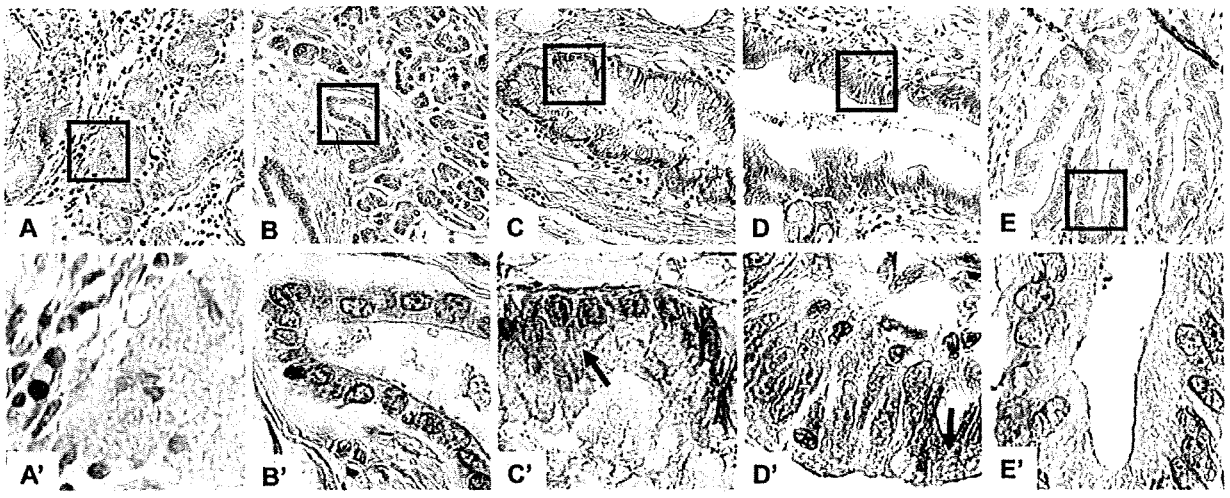

Fig. 7 Immunohistochemical staining for COX-1 in resected BD-IPMN specimens. Staining of gastric gland and mononuclear cell of gastritis mucosa for positive control (**a**). Representative specimens of normal epithelium (**b**), hyperplasia (**c**), adenoma (**d**), and carcinoma (**e**). High magnification images of the *boxed area* from **a** to **e** were shown in **a′**–**e′**. Normal epithelium showed no staining at all and was scored as 0. Perinuclear area of hyperplasia and adenoma slightly stained brownish (*arrows* in **c′** and **d′**), but because the staining was present only in a limited area, the score was 0. Carcinoma showed no staining at all and was scored as 0. ×200 in **a**–**e**, 1,000 × in **a′**–**e′**

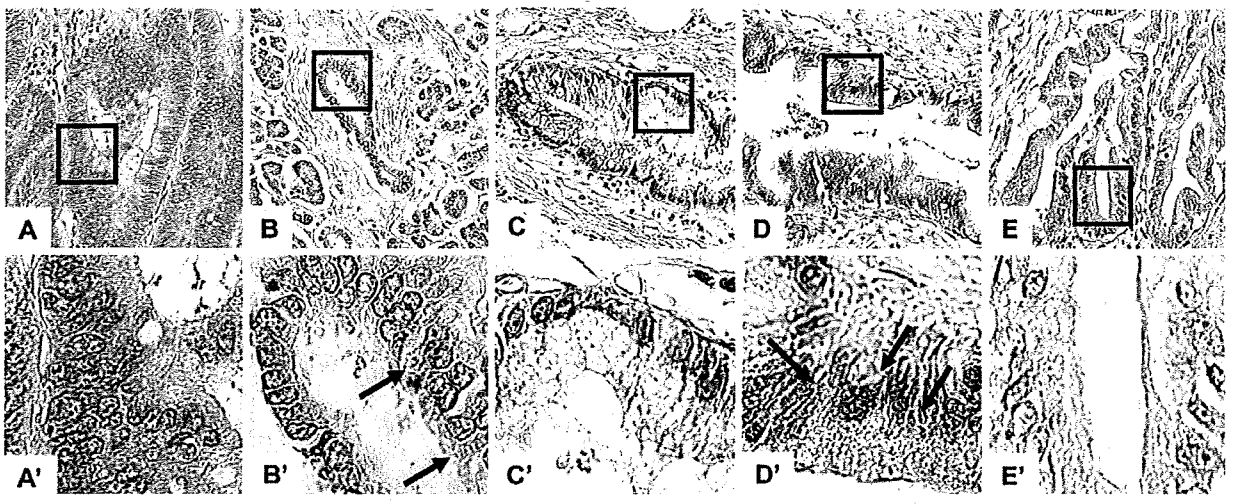

Fig. 8 Immunohistochemical staining for COX-2. Staining of colonic carcinoma tissue for positive control (**a**). Serial sections of BD-IPMN specimens in Fig. 7 (**b–e**). High magnification images of the *boxed area* from **a** to **e** were shown in **a′–e′**. The cytoplasm of normal epithelium stained light brownish (*arrows* in **b′**) only in a limited area and was scored as 0; hyperplasia did not stain at all and was scored as 0; up to half of the area of cytoplasm of adenoma stained light brownish (*arrows* in **d′**) and was scored 2; and carcinoma did not stain at all and was scored as 0. ×200 in **a–e**, ×1,000 in **a′–e′**

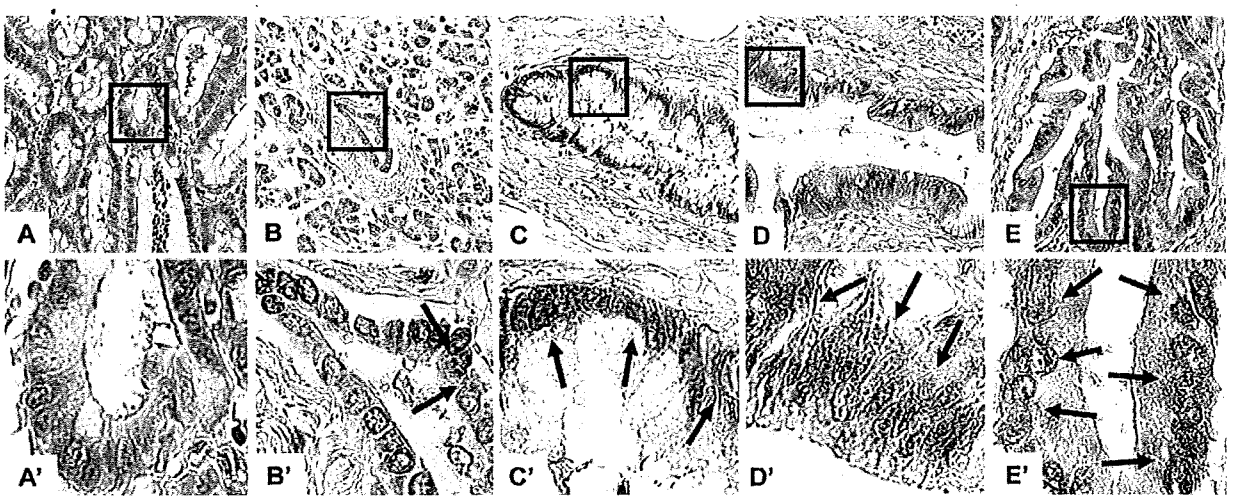

Fig. 9 Immunohistochemical staining for GST-π. Staining of colonic carcinoma tissue for positive control (**a**). Serial sections of BD-IPMN specimens in Fig. 7 (**b–e**). High magnification images of the *boxed area* from **a** to **e** were shown in **a′–e′**. The perinuclear area of normal epithelium stained light brownish (*arrows* in **b′**), but because the area of staining was limited, was scored 0; hyperplasia and adenoma were scored as 8 based on the finding that the nucleus and cytoplasm were both stained brown throughout the lesion (*arrows* in **c′** and **d′**); and carcinoma was scored as 3 because the staining intensity of nucleus and cytoplasm was low and the area showing light brown staining included more than half of the whole lesion (*arrows* in **e′**). ×200 in **a–e**, ×1,000 in **a′–e′**

(Fig. 6a), communication of the branch duct to the main pancreatic duct (white bracket, Fig. 6b), filling defect in the main pancreatic duct (white arrow, Fig. 6b), and a multilocular cyst (white bracket, Fig. 6c), consistent with imaging findings of BD-IPMNs. During the observation period, though the maximum branch duct diameter remained nearly stationary (white bracket, Fig. 6c–e), one of the branched cysts (white arrowhead, Fig. 6c–e) clearly increased in size. EUS revealed the growth of mural nodules from 7 mm (white arrowhead, Fig. 6f) to 9 mm (white arrowhead, in Fig. 6g) after 6 months.

Immunohistochemical staining of COX-1, COX-2 and GST-π in BD-IPMN tissues

In exploring the putative target molecule for sulindac, we performed immunohistochemical staining of COX-1, COX-2 and GST-π in BD-IPMN tissues from eight

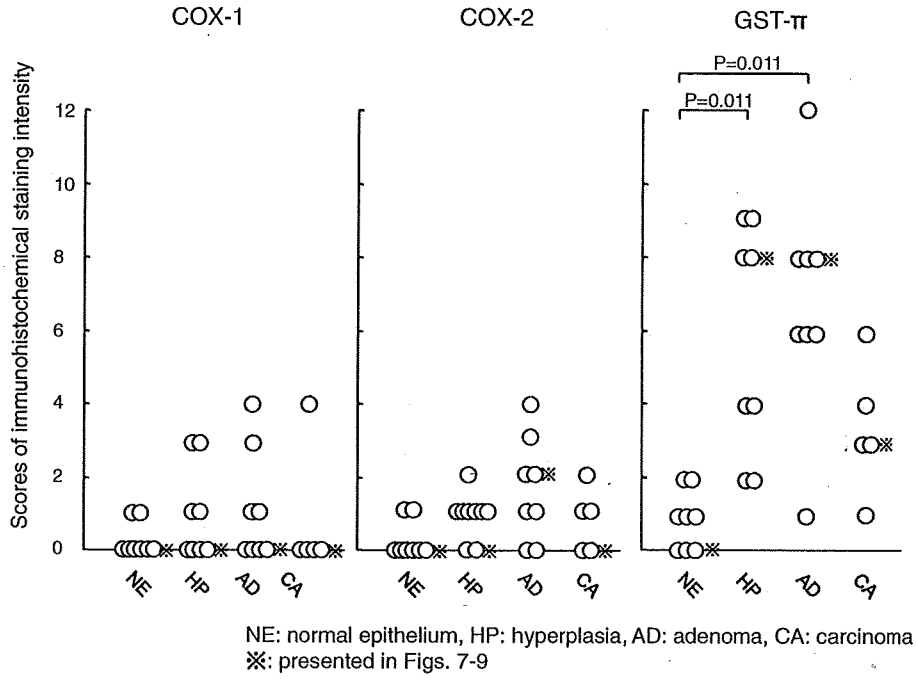

Fig. 10 Scores of immunohistochemical staining intensity for COX-1, COX-2 and GST-π in normal epithelium, hyperplasia, adenoma and carcinoma. Scoring was made according to the method of Gong et al

non-study patients who had undergone surgical resection of the pancreas because of malignant imaging signs. Of the eight resected tissues, portions of five consisted of carcinoma, adenoma and hyperplasia and portions three of adenoma and hyperplasia.

Typical immunohistochemical staining patterns for COX-1, COX-2 and GST-π in specimens from patients whose BD-IPMNs tissue was admixed with portions of carcinoma, adenoma and hyperplasia are shown in Figs. 7, 8, and 9, respectively. Staining of COX-1 (Fig. 7) and COX-2 (Fig. 8) was very faint, if at all, in specimens that included hyperplasia (c), adenoma (d) and carcinoma (e) with intensity similar to that in the normal epithelial portion (b). In contrast, staining for GST-π (Fig. 9) was evident in the specimen with hyperplasia (c), adenoma (d) and carcinoma (e) in contrast to the almost negative staining of the normal epithelium (b). When we quantified the staining intensity of all the specimens examined according to the method of Gong et al. [19] the scores of COX-1 and COX-2 in hyperplasia and adenoma were at most three with no difference compared to that of normal epithelium, while staining intensity of GST-π in hyperplasia and adenoma scored significantly higher compared to that of normal epithelium ($P = 0.011, P = 0.011$) (Fig. 10). Statistical comparison of scores for COX-1, COX-2 and GST-π in carcinoma to those of normal epithelium, hyperplasia or adenoma could not be made because carcinoma was seen in only five of the eight resected pancreases while other lesions and normal epithelial portions were present in all eight specimens.

Discussion

In forming the treatment group for the present study, for ethical reasons we assigned only those patients who rejected undergoing operation even though their lesions or symptoms met the criteria of the IAP for surgical resection. The control group was comprised of 10 patients whose lesion did not meet the IAP criteria for surgical resection and one patient (case 11) who had a history of asthma in response to NSAIDs, although her lesion met the operation criteria. Therefore, the study was neither randomized nor controlled. However, we believe that the comparison of changes between the groups was reasonable to examine the effect of sulindac since the branch duct diameter in the treatment group was generally larger than in the control group. Thus, the results showing that the branch duct diameter was significantly reduced after 18 months of treatment with sulindac compared to the change in diameter during the natural course in the control group suggested that chemoprevention held promise for treatment of BD-IPMNs.

However, when we compared the effect of the drug treatment on branch ducts with that on mural nodules in each case, we found a discrepancy. In cases 5, 6, and 9, the height of the mural nodules decreased while the branch duct diameter was unchanged during the course of treatment. The discrepancies between the mural nodule height and branch duct diameter in each case were also observed in the lesions prior to treatment (Table 1).

Those lesions having relatively large mural nodules, as in cases 1, 8 and 10, had relatively small branch ducts while lesions with no mural nodule (case 4) or with a very tiny nodule (case 5) had an obviously dilated branch duct. Such a discrepancy may be explained by the assumption that production rates of mucin are different in each mural nodule and that the draining rates of mucin to the main pancreatic duct from branch ducts are different in each case. A small mural nodule could produce a relatively large amount of mucin and the drainage of mucin from the branch duct of a lesion with a large mural nodule could be very rapid. Thus, the branch duct diameter does not necessarily reflect the mural nodule height. This is compatible with the previous notion that an increase in branch duct diameter does not necessarily indicate malignancy or tumor progression [20, 21]. In this context, data on mural nodule height are considered to be more reliable than those on branch duct diameter. Unfortunately, analysis of mural nodule height in the control group was performed by the Wilcoxon signed-rank test because data on some patients for 6 months (cases 13, 17, 19, and 22) and on all patients for 18 months were lacking. However, when we employed the Friedman test on the treatment group, the suppressive effect on nodule height was evident. Incidentally, in our study, one out of seven patients (14.3%) in control group who underwent EUS monitoring developed a new mural nodule. This ratio is apparently higher than that (4.9%) reported by Tanno et al. [20] who followed up 82 mural nodule free BD-IPMN cases for 45–148 months. This discrepancy may be due to the fact that number of our cases was relatively small as compared to that of Tanno's study.

The finding that the main pancreatic duct diameter was not affected by the treatment may be due to the fact that patients with dilated MPD (>6 mm), which is the sign for tumor invasion to the MPD, were not enrolled in this study. Nevertheless, collectively the present results on both branch duct diameter and mural nodule height of BD-IPMNs are indeed supportive of legitimate grounds for utilization of drugs to prevent carcinoma which may be derived from BD IPMNs. Further more, since it has been recently reported that BD-IPMNs are not infrequently associated with ductal carcinoma and that mucous cell hyperplasia harboring K-ras mutation which is one of the histological differentiation in the adenoma-carcinoma sequence of IPMNs might be a background for the development of ductal carcinoma [22], chemopreventive modality may also be effective on such ductal carcinoma. However, long term and larger scale follow up study should be established in future to conclude the feasibility of chemoprevention for both carcinoma derived from BD-IPMNs and ductal carcinoma.

Because we used omeprazole in addition to sulindac in the treatment group and not in the control group, we cannot single out sulindac as the sole drug causing the effect that we observed. However, previous reports have suggested that sulindac suppresses cell proliferation or induces cell apoptosis and that omeprazole rather exerts cytoprotective activity; therefore, we believe that sulindac is the principal drug that exerted the suppressive effect on the nodules [11, 12, 23].

The target molecule of sulindac is known to be COX-1 and COX-2 and hence we explored expression of those enzymes in IPMNs. To our surprise, however, unlike findings of a previous report [24], our study showed that neither COX-1 nor COX-2 was overexpressed in both the premalignant and malignant portions of BD-IPMNs. Instead, GST-π, a second class detoxification enzyme overexpressed in many precancerous lesion as well as in cancer tissue [25], was clearly stained in hyperplasia, adenoma and carcinoma associated with BD-IPMNs. Because we have recently found that GST-π knock-out mice rarely develop colonic cancer (unpublished observation) and that sulindac inhibited activity of GST-π in vitro [23], it is highly plausible that the target molecule of sulindac in IPMNs may also be GST-π. A future clinical trial using a GST-π-specific inhibitor may clarify the validity of this speculation.

In conclusion, results of the present study suggested the usefulness of chemoprevention of carcinoma derived from BD-IPMNs by sulindac, at least in those patients who refused surgery even though their lesions met the criteria for surgical resection. However, to confirm our present observation, a randomized controlled study with a larger number of patients is certainly needed.

References

1. Nakagohri T, Kenmochi T, Kainuma O, Tokoro Y, Asano T. Intraductal papillary mucinous tumors of the pancreas. Am J Surg. 1999;178:344–7.
2. Terris B, Ponsot P, Paye F, Hammel P, Sauvanet A, Molas G, et al. Intraductal papillary mucinous tumors of the pancreas confined to secondary ducts show less aggressive pathologic features as compared with those involving the main pancreatic duct. Am J Surg Pathol. 2000;24:1372–7.
3. Kobari M, Egawa S, Shibuya K, Shimamura H, Sunamura M, Takeda K, et al. Intraductal papillary mucinous tumors of the pancreas comprise 2 clinical subtypes: differences in clinical characteristics and surgical management. Arch Surg. 1999;134:1131–6.
4. Doi R, Fujimoto K, Wada M, Imamura M. Surgical management of intraductal papillary mucinous tumor of the pancreas. Surgery. 2002;132:80–5.
5. Matsumoto T, Aramaki M, Yada K, Hirano S, Himeno Y, Shibata K, et al. Optimal management of the branch duct type intraductal papillary mucinous neoplasms of the pancreas. J Clin Gastroenterol. 2003;36:261–5.
6. Tanaka M, Chari S, Adsay V, Fernandez-del Castillo C, Falconi M, Shimizu M, et al. International Association of Pancreatology